

Review

Open Access



Constructing and regulating nanochannels in two-dimensional-material-based membranes for specified separation applications

Chao Xing^{1,2,#}, Mengchen Zhang^{1,#}, Lingfeng Liu¹, Zehua Zheng¹, Ming Zhou², Shanqing Zhang² , Changyu Liu¹ 

¹School of Biotechnology and Health Sciences, Wuyi University, Jiangmen 529020, Guangdong, China.

²Centre for Catalysis and Clean Energy, School of Environment and Science, Gold Coast Campus, Griffith University, Queensland, QLD 4222, Australia.

[#]Authors contributed equally to this work.

Correspondence to: Prof. Shanqing Zhang, Centre for Catalysis and Clean Energy, School of Environment and Science, Gold Coast Campus, Griffith University, Queensland, QLD 4222, Australia. E-mail: s.zhang@griffith.edu.au; Dr. Ming Zhou, Centre for Catalysis and Clean Energy, School of Environment and Science, Gold Coast Campus, Griffith University, QLD 4222, Queensland, Australia. E-mail: ming.zhou@griffith.edu.au; Prof. Changyu Liu, School of Biotechnology and Health Sciences, Wuyi University, Jiangmen 529020, Guangdong China. E-mail: wyuchemistry@126.com

How to cite this article: Xing C, Zhang M, Liu L, Zheng Z, Zhou M, Zhang S, Liu C. Constructing and regulating nanochannels in two-dimensional-material-based membranes for specified separation applications. *Microstructures* 2023;3:2023031. <https://dx.doi.org/10.20517/microstructures.2023.11>

Received: 26 Feb 2023 **First Decision:** 19 Apr 2023 **Revised:** 26 May 2023 **Accepted:** 2 Jun 2023 **Published:** 10 Jul 2023

Academic Editors: Shujun Zhang, Yi Du **Copy Editor:** Fangyuan Liu **Production Editor:** Fangyuan Liu

Abstract

The two-dimensional (2D) materials offer atomic-level thickness and unique physical and chemical properties for the preparation of a new class of membranes, i.e., nanochannel membranes. The nanochannel membranes have been utilized in a broad spectrum of new separation applications. However, the instability of the nanochannels, interfacial instability of 2D materials, and the swelling problem could damage the membrane performance, such as permeability, selectivity, and service lifetime. Innovative strategies for constructing and regulating the nanochannels are enthusiastically explored to address these challenges. Along this line, in this work, we first provide insight into the mechanisms of the nanochannel construction, the separation mechanism, and the effect of nanochannels on the separation performance. Then, the strategies developed in the literature, in particular, the strategies for the preparation of ideal 2D nanosheets, the strategies for constructing nanochannels, and the strategies for regulating the characteristics of nanochannels (channel size, channel length, channel morphology, and channel surface physicochemical properties) are systematically summarized. After that, we briefly introduce the application of 2D-material-based nanochannel membranes and outline the current challenges and provide an



© The Author(s) 2023. **Open Access** This article is licensed under a Creative Commons Attribution 4.0 International License (<https://creativecommons.org/licenses/by/4.0/>), which permits unrestricted use, sharing, adaptation, distribution and reproduction in any medium or format, for any purpose, even commercially, as long as you give appropriate credit to the original author(s) and the source, provide a link to the Creative Commons license, and indicate if changes were made.



outlook in the further exploration of separation mechanism, large-scale manufacturing, and the eventual commercialization of the membranes.

Keywords: 2D nanosheet, nanochannel, membrane, separation, regulation, construction

INTRODUCTION

Membrane separation technologies have become revolutionized various industries by offering numerous benefits, such as low cost, high efficiency, and environmental sustainability. These technologies utilize thin membrane barriers that separate specific substances based on variations in size, charge, or other properties. Membranes can be roughly categorized into macrochannel membranes, microchannel membranes, and nanochannel membranes, depending on the size of the channels and their characteristic scale. Macrochannel membranes possess larger channel dimensions, typically in the millimeter to centimeter range. They are designed for applications involving larger particles or higher flow rates and are commonly used in pre-treatment processes in various industries, including chemical, environmental, pharmaceutical, mining, and more. Microchannel membranes have smaller channel dimensions than macrochannels but are still relatively large when compared to nanochannels. Typically, their channel sizes range from tens to hundreds of microns in diameter. They find a variety of applications in areas such as microfluidics, chemical synthesis, and biomedical devices. Nanochannel membranes feature channels with dimensions typically in the nanometer range. These membranes are engineered with extremely small channel sizes to precisely control molecular or ion transport. They are extensively used in diverse applications such as water treatment, ion selectivity, gas separation, DNA sequencing, protein analysis, drug delivery systems, *etc.* Each scale of the membrane has its own strengths and weaknesses (as shown in [Table 1](#) below), and the choice of the membrane depends on the specific separation requirements, target molecules or ions, and operating conditions^[1-7].

Compared with other membranes, nanochannel membranes have unique advantages due to their extremely small channel size, offering the potential for highly selective separations, reduced sample consumption, and single-molecule analysis. These properties make nanochannel membranes particularly suitable for applications that require precise control of molecular transport and analysis and have received increasing attention from the scientific and engineering communities^[8-14]. To meet specific requirements, ultrathin nanochannel membranes can be directly assembled from a variety of inorganic or organic materials. Two-dimensional (2D) materials are of particular interest in the field of nanochannel engineering due to their unique physical and chemical properties, including atomic-level thickness, hydrophilicity, and ductility. A diverse range of 2D materials are currently under investigation, such as graphene^[15], graphene oxide (GO)^[16], transition metal carbides/nitrides (MXenes)^[17], hexagonal boron nitride (h-BN)^[18], graphitic carbon nitride (g-C₃N₄)^[19], transition metal dichalcogenides (TMDs)^[20,21], layered double hydroxides (LDHs)^[22], 2D zeolites^[23], 2D metal-organic frameworks (2D MOFs)^[24], 2D covalent organic frameworks (2D COFs)^[25], and beyond. These materials offer a wealth of possibilities for creating high-performance 2D-material-based nanochannel membranes. The superb separation performance achieved by nanochannel membranes based on 2D materials is mainly attributed to the unique properties and structural characteristics of the materials. The atomic-level thickness of 2D materials allows the formation of nanochannels with precise dimensions, which can effectively restrict the passage of certain molecules or ions depending on their size. In addition, the layer spacing and surface chemistry of the nanochannels can be modulated by introducing functional groups or modifying the surface, further affecting the selectivity of the membrane. In addition, the high aspect ratio and large surface area of 2D materials provide abundant active sites for interaction with the target material, thus enabling molecular sieving and preferential ion transport. In addition, the ordered arrangement of nanosheets in the membrane structure facilitates the formation of continuous and uniform

Table 1. Key characteristics of macrochannel, microchannel, and nanochannel membranes

Membrane type	Channel size (typical range)	Key features	Applications
Macrochannel	> 100 μm	Large channel size, low surface-to-volume ratio, turbulent flow regime, and reduced resistance to flow	Pre-treatment processes in chemical, environmental, pharmaceutical, mining, and other industries
Microchannel	1-100 μm	Intermediate channel size, moderate surface-to-volume ratio, laminar flow regime, and diffusion dominates	Microfluidics, lab-on-a-chip devices, chemical synthesis, and separation processes
Nanochannel	< 100 nm	Very small channel size, high surface-to-volume ratio, molecular selectivity, and electrostatic interactions dominate	Water treatment, ion selectivity, gas separation, DNA sequencing, single-molecule analysis, nanofluidics, and biosensors

nanochannels, which improves permeation efficiency. Overall, the combination of these factors allows 2D-material-based nanochannel membranes to achieve selective separations by exploiting the size, charge, and interaction-based properties of the target species.

To comprehensively assess the performance of the membranes, several formulas can be utilized, including the rejection coefficient, separation factor, permeability, flux, rejection, fouling index, and interlayer spacing. By quantifying these parameters, researchers can better understand the potential benefits of using 2D materials with densely packed nanochannels for nanoscale separation applications.

The rejection coefficient (R) is determined by equation (1), where C_{feed} is the solute concentration in the feed, and $C_{permeate}$ is the solute concentration in the permeate.

$$R = \frac{C_{feed} - C_{permeate}}{C_{feed}} \quad (1)$$

The separation factor (α) is defined as the ratio of the rejection coefficients of two different solutes, A and B, which is determined by equation (2).

$$\alpha = \frac{R_A}{R_B} \quad (2)$$

Permeability (P) measures the ease with which a solvent flow through a porous material and is calculated using the formula (3), where Q is the permeate volume, A is the effective membrane area, and ΔP is the transmembrane pressure.

$$P = \frac{Q}{(A \times \Delta P)} \quad (3)$$

Flux (J) represents the volume of permeate that passes through the membrane per unit area per unit of time and is calculated using the formula (4), where Δt is the time.

$$J = \frac{Q}{A \times \Delta t} \quad (4)$$

Rejection (Re_j) is defined as the ratio of the solute concentration in the feed to the solute concentration in the permeate and is calculated using the formula (5).

$$Rej = 1 - \frac{C_{permeate}}{C_{feed}} \quad (5)$$

The fouling index (*FI*) is calculated using the formula (6), where J_{clean} is the flux of the clean membrane, and J_{fouled} is the flux of the fouled membrane.

$$FI = \frac{J_{clean} - J_{fouled}}{J_{clean} \times 100\%} \quad (6)$$

The interlayer spacing of the 2D-material-based nanochannel membranes can be calculated using the Bragg equation for X-ray diffraction (XRD), which is given by formula (7), where d is the interlayer spacing, λ is the wavelength of the X-ray, and θ is the diffraction angle.

$$d = \frac{\lambda}{2 \sin \theta} \quad (7)$$

Through a comprehensive analysis of membrane performance using the equations outlined above, valuable insights can be gained into the potential of nanochannel membranes based on 2D materials with densely packed channel arrays. These membranes are anticipated to offer several distinct advantages for nanoscale separation applications, including the following: (1) The membranes possess simple and tunable nanochannels that facilitate quantitative modeling and probing of nanofluids transport mechanisms; (2) The membranes allow flexible modification of nanochannels with favorable functionality to meet various application requirements; (3) The membranes enable ultra-thin structures down to single-atom thickness and ultra-high throughput by simple and scalable methods; and (4) The membranes can provide nanochannels with specific sizes, and the size can be precisely controlled from tens of nanometers to sub-nanometer scale to achieve high selectivity^[5,26,27].

Although their numerous theoretical advantages, 2D-material-based nanochannel membranes still face many practical challenges. One such challenge is that most 2D materials, including GO and MXene, contain numerous hydroxyl groups, carboxyl groups, Ti-O, and other hydrophilic functional groups on their surfaces, which can lead to severe swelling problems and thus reduce the selectivity of the membranes^[28]. Additionally, interfacial instability of 2D materials makes membrane structures very prone to collapse, resulting in generally shorter membrane lifespans that cannot meet practical needs^[29]. Besides, high operating pressures are still required for some membranes to achieve high permeability, which leads to increased energy consumption, and other issues such as poor anti-fouling ability and relatively expensive construction costs must be addressed^[30]. Given these challenges, there is no consensus on whether developing innovative, large-scale reproducible strategies for constructing and regulating nanochannels is a top priority for solving the aforementioned problems and ultimately enabling the widespread use of membranes in industrial applications. Most of the reviews in the literature focus more on the intricate details of membrane construction, regulation, and the role of nanochannels in separation performance. In contrast, this work seamlessly links the separation mechanisms, addressing the nanochannel separation and collapsing issues, selection of suitable membranes, and various practical applications.

This comprehensive review delves into the intricate details of membrane construction and regulation, highlighting the critical role of nanochannels in separation performance. This insight into the mechanism behind nanochannel collapse also provides invaluable insight into choosing the most suitable membrane for a particular application. As the fundamental building “bricks” of membrane construction, obtaining the ideal 2D material is a crucial starting step for achieving high-performance membranes. Therefore, the

review begins with a comprehensive description of 2D-material preparation strategies, including “top-down” and “bottom-up” approaches. Nanochannel properties directly impact separation performances, such as permeability and selectivity, and as such, the review outlines 2D nanosheet perforation methods (i.e., drilling out-of-plane nanochannels, similar to creating “porous bricks”) and membrane assembly methods (similar to building “house”) for obtaining in-plane nanochannels. Nanochannel regulation is similar to “renovating a house”, giving the membrane improved structural and functional properties. Thus, four aspects of such modification are briefly discussed (i.e., channel size, channel length, channel morphology, and surface chemistry). Laboratory-scale application attempts are the first step towards industrial applications (similar to “trial residence”), which are also reviewed. Afterward, to give readers a more intuitive picture, the review also categorizes various representative application scenarios and describes their specific needs for membranes, such as liquid molecular separation, gas separation, and ion sieving. A visual summary of the main elements described above is provided in [Figure 1](#). In the final section, we conclude with a discussion of current challenges and an outlook on the eventual commercialization of membranes. Overall, this comprehensive review presents readers with a detailed roadmap of the entire process of membrane preparation and regulation from raw materials to final applications (“clay” to “bricks” to “furnished houses”) and highlights the corresponding strategies employed in each step. By providing clear and concise information, this review aims to inspire future research and the development of new and innovative membrane preparation and regulation strategies, ultimately leading to the realization of highly efficient and effective membrane technologies.

CONSTRUCTING NANOCHANNELS WITH 2D NANOSHEETS

2D nanosheets refer to a class of materials that consists of only one or a few atomic layers, exhibiting an ultrathin sheet-like geometry beyond the nanoscale^[31]. These materials are characterized by strong interlayer covalent bonds and weak interlayer van der Waals bonds and exhibit excellent electrical, optical, and mechanical properties compared to their bulk counterparts, making them extremely attractive in the fields of physics, materials science, and chemistry^[32]. The successful isolation of monolayer graphene by Novoselov *et al.* in 2004 paved the way for the exploration of many other 2D materials, which have become ideal building blocks for the development of membranes with nanochannels due to their atomic thickness and unique physicochemical properties^[30,33].

When 2D materials are engineered into membranes, two basic forms of nanochannels can be created: out-of-plane nanochannels and in-plane nanochannels. Out-of-plane nanochannels can be formed by utilizing 2D nanosheets with intrinsically porous or perforating intrinsically nonporous 2D materials. In-plane nanochannels can be fabricated from 2D layered membranes in which several or multiple layers of nanosheets are aligned parallel to form well-defined nanochannels. This section describes typical construction strategies for creating nanochannels from 2D materials, including synthetic methods for intrinsic nanopores by multilayer peeling or monolayer growth, perforation approaches for artificial nanopores through physical and chemical etching, and various membrane assembly methods, including van der Waals assembly of individual nanochannels through nanosheet extraction, solution-assisted assembly of dense nanochannels by pressure/vacuum filtration, spin/spray coating, and other techniques.

Synthesis of 2D nanosheets

2D nanosheets serve as the foundational materials for constructing nanochannels from 2D materials. The synthesis of 2D nanosheets can be generally classified as “top-down” and “bottom-up” strategies, as shown in [Figures 2 and 3](#).

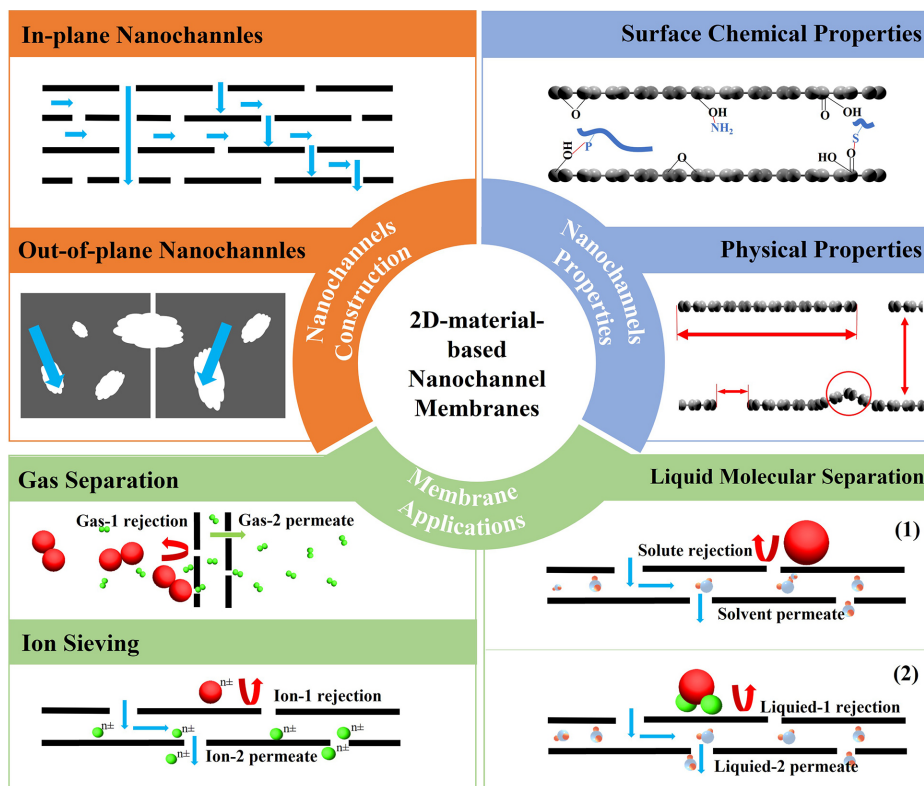


Figure 1. Strategies for constructing nanochannels, regulating nanochannels, and applications of 2D-material-based nanochannel membranes.

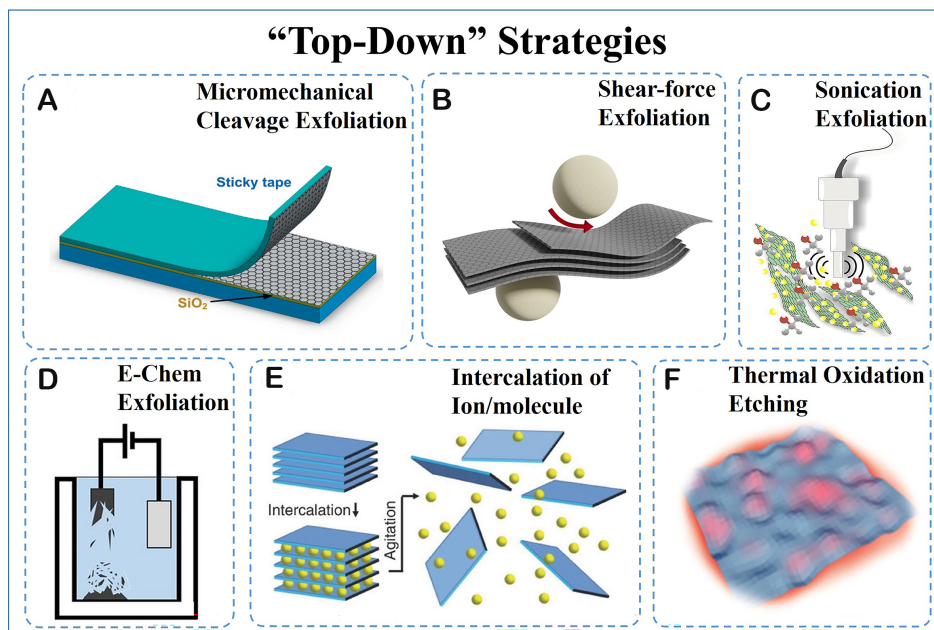


Figure 2. Schematics of the main “top-down” synthesis strategies of 2D nanosheets. (A) Micromechanical cleavage exfoliation^[171]. Copyright 2012, Elsevier Ltd. (B) Ball milling shear-force exfoliation. (C) Sonication exfoliation^[172]. Copyright 2018, Elsevier B.V. (D) Electrochemical (E-Chem) exfoliation^[38]. Copyright 2018, Springer Nature. (E) Ion/molecule intercalation^[173]. Copyright 2017, John Wiley & Sons, Inc. (F) Thermal oxidation etching^[47]. Copyright 2021, John Wiley & Sons, Inc.

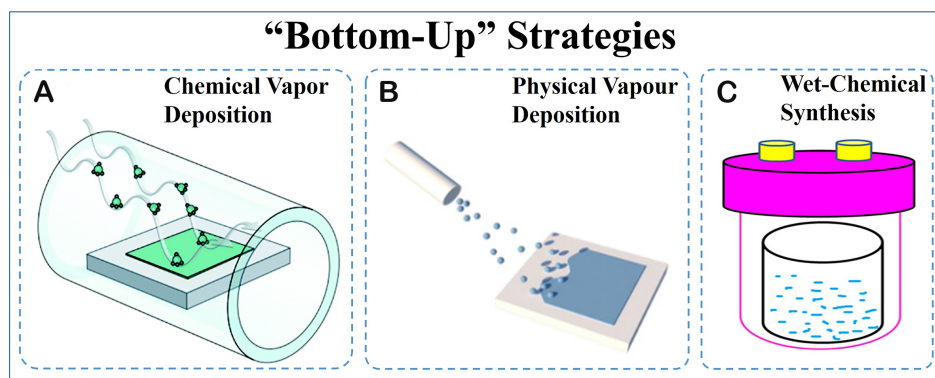


Figure 3. Schematics of the main “bottom-up” synthesis strategies of 2D nanosheets. (A) Chemical vapor deposition^[174]. Copyright 2017, Springer Nature. (B) Physical vapor deposition^[47]. Copyright 2021, John Wiley & Sons, Inc. (C) Wet-chemical synthesis^[175]. Copyright 2021, American Chemical Society.

The “top-down” strategy involves the exfoliation of 2D nanosheets from bulk-layered materials by breaking weak interlayer van der Waals, π - π stacking, and/or hydrogen bonding interactions [Figure 2]. Novoselov *et al.* pioneeringly achieved a single layer of graphite using the micromechanical cleavage method [Figure 2A], which enables the preparation of a variety of 2D nanosheets with a clean surface and high quality on a macroscopic scale^[33,34]. However, it is worth noting that this method has the drawback of low efficiency. Paton *et al.* took the lead in conducting shear force-assisted^[35] [Figure 2B] and sonication-assisted^[36] [Figure 2C] exfoliations in liquids, where bulk graphene and TMDs crystals can be efficiently dispersed in common solvents to obtain large quantities of mono- and few-layer nanosheets. Another representative shear force-assisted and sonication-assisted mixed work is demonstrated by Peng *et al.*, who developed a soft-physical process of preparing 2D MOF nanosheets with large lateral sizes by low-energy wet ball milling coupled with ultrasonication in methanol/propanol mixtures^[37]. Electrochemical (E-Chem) exfoliation [Figure 2D] is a promising bulk method for producing graphene from graphite, where an applied voltage drives ionic species to intercalate into graphite, forming gaseous species that expand and exfoliate individual graphene sheets. Achee *et al.* reported a method for sustained graphene output within a permeable and expandable containment system, indicating both high yield (65%) and extraordinarily large lateral size ($> 30 \mu\text{m}$) of graphene^[38].

The use of specific ions or molecules intercalation [Figure 2E] to weaken interactions within the layers by exchanging or reacting can further enhance the efficiency of liquid-phase exfoliations, which have been widely employed for preparing various types of 2D nanosheets such as GO, MXene, TMDs, and LDHs^[39-42]. Notably, these intrinsically nonporous 2D nanosheets still require a subsequent perforation process to fabricate nanochannels (as discussed in the next section). For example, intrinsically porous 2D nanosheets can be exfoliated from their related layered materials with high purity via melt blending with a polymer matrix, as demonstrated by Varoon *et al.*^[43]. And the synthesis of g-C₃N₄ nanosheets can be achieved by thermal oxidation [Figure 2F] with long-time heating and etching, which was shown by Ren *et al.*, to produce a series of g-C₃N₄ nanosheets with a thinner layer thickness, larger BET surface area, and higher graphitic nitrogen ratio^[44]. They proposed that the higher activity of the g-C₃N₄ from long-time thermal oxidative etching might be ascribed to the enlarged specific surface, pore volume, and higher graphitic nitrogen ratio with the loose and soft laminar morphology^[44].

However, it should be noted that the “top-down” strategy for exfoliation is limited by the availability of layered materials, which may result in incidental structural deterioration and morphological damage during

the exfoliation process. Such issues may hinder the obtainment of ideal 2D nanosheets.

The “bottom-up” strategy [Figure 3] involves synthesizing 2D nanosheets through chemical reactions from specific precursors under given conditions, which is theoretically feasible for all types of 2D nanosheets. Chemical vapor deposition (CVD) [Figure 3A] growth and physical vapor deposition (PVD) [Figure 3B] growth are reliable routes for synthesizing highly crystalline 2D nanosheets such as graphene, MXene, h-BN, TMDs, and others, with large-area uniformity^[45-47]. However, transferring the crack-free as-prepared 2D nanosheets from the substrate remains challenging^[48-50]. As an alternative, wet-chemical synthesis [Figure 3C] is widely employed due to its good controllability, reproducibility, and scalability, especially for preparing those crystalline porous materials made from predesigned skeletons such as zeolites, MOFs, and COFs. Jeon *et al.* successfully produced high-aspect-ratio MFI-type zeolite nanosheets using a nanocrystal-seeded growth method that was triggered by a single rotational intergrowth^[51]. These highly oriented MFI nanosheets with straight vertical micropores allow the secondary growth of thin and defect-free MFI membranes with extraordinary performance for separating xylene isomers^[51]. Makiura *et al.* reported a procedure for the rational modular assembly of MOF nanosheets with perfect orientation on a solid substrate by integrating the layer-by-layer growth and the Langmuir-Blodgett methods^[52]. Similarly, Rodenas *et al.*^[53] presented a new approach to produce self-standing intact MOF nanosheets that relied on the diffusion-mediated modulation of the MOF growth kinetics. The synthesis medium involves three vertically arranged liquid layers, where a topmost solution of cations and a bottom solution of linker precursors diffuse into the intermediate solvent layer, causing a slow supply of the MOF nutrients to form MOF nanosheets in a highly diluted medium. On the other hand, COF nanosheets can either grow on various substrates under solvothermal conditions or at solid-liquid/liquid-liquid/air-liquid interfaces via interfacial polymerizations^[54,55]. An excellent representative work was done by Kandambeth *et al.*, who successfully demonstrated the fabrication of various flexible, continuous, and defect-free COFs by casting and baking the mixed solution containing organic linkers and co-reagents^[56]. In addition, the “bottom-up” approach can also be used to directly fabricate porous graphene with a well-defined pore structure by selecting appropriate rigid molecular building blocks as monomers for the organic synthesis^[57].

Perforation on 2D nanosheets

Unlike intrinsically porous 2D nanosheets, the perfect monolayer nonporous 2D nanosheets are almost impermeable, requiring the artificial drilling of out-of-plane nanoscale holes to serve as nanochannels. Continuous experimental endeavors have been made to develop various perforation techniques to realize this goal, including physical and chemical methods such as focused electron beam, bombardment/focused ion beam, oxygen plasma etching, ultraviolet-induced oxidative etching, and chemical etching [Figure 4]. For example, Fischbein *et al.* showed that graphene nanosheets could be controllably nano-sculpted using the focused electron beam ablation technique with few nanometer precisions [Figure 4A]^[58]. Similarly, Koenig *et al.* utilized ultraviolet-induced oxidative etching [Figure 4B] to create angstrom-sized pores in the pristine graphene membrane, which were used as molecular sieves and exhibited selective gas transport capabilities^[59].

The focused ion beam perforation method is another effective technique [Figure 4C], which was successfully employed by Celebi *et al.* to produce narrowly-distributed pore sizes ranging from < 10 nm to 1 μm in free-standing graphene^[60]. Later, Russo *et al.* created pore nucleation sites on graphene using an argon ion beam followed by edge-selective electron recoil sputtering, yielding graphene nanopores with radii as small as 3 \AA , all without the use of focused beams^[61]. However, the effective areas of these nanoporous graphenes are limited to the micrometer scale. To overcome this limitation, O'Hern *et al.* introduced isolated and reactive defects into the graphene lattice through ion bombardment, which were then enlarged by oxidative etching to produce permeable pores with diameters of 0.40 ± 0.24 nm and

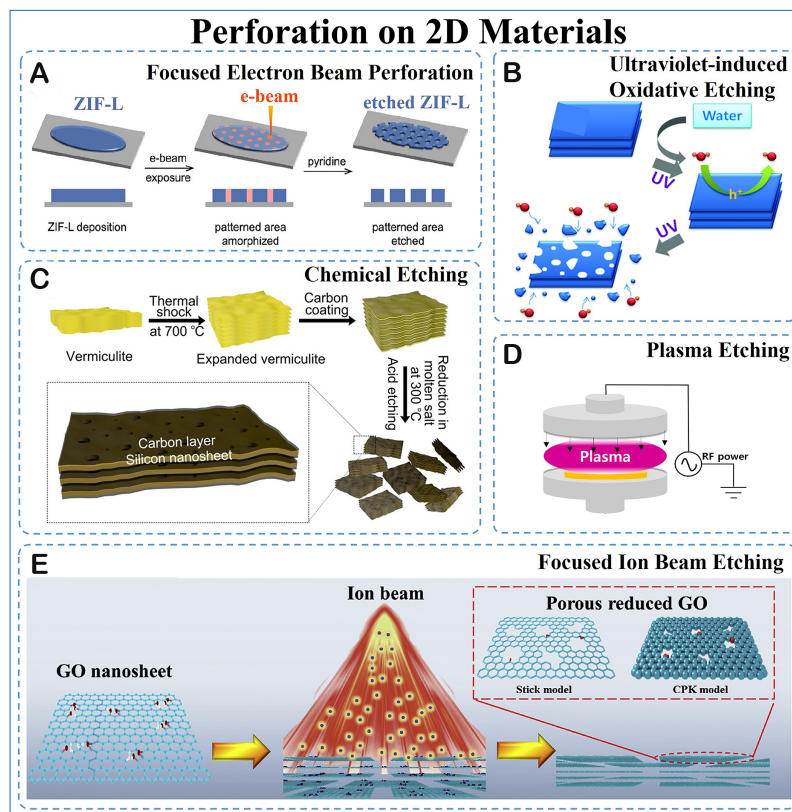


Figure 4. Schematics of perforation on 2D materials. (A) Low-dose e-beam patterning of ZIF-L with pyridine as an etchant^[176]. Copyright 2021, American Chemical Society. (B) UV irradiation etching of MoS₂/WS₂ nanosheets^[177]. Copyright 2016, Royal Society of Chemistry. (C) Focused ion beam etching process on GO^[178]. Copyright 2019, Elsevier Ltd. (D) Plasma etching process^[179]. Copyright 2020, MDPI. (E) The synthesis of porous Si/C composite nanosheets by chemical etching^[180]. Copyright 2019, American Chemical Society.

densities exceeding 10^{12} cm^{-2} ^[62]. In another approach, Surwade *et al.* employed an oxygen plasma etching process [Figure 4D] to produce nanopores with tunable diameters on a graphene monolayer, which exhibited rapid water transport and excellent salt rejection^[15]. Despite the success of these methods in achieving tailored pore sizes and densities, they can be relatively expensive due to the use of specialized instruments.

Generally, physical etching is an effective method to prepare arrays of monodisperse nanopores with a precise and tunable pore size distribution, whereas chemical etching [Figure 4E] is relatively easy and low-cost to produce nanopores in the graphene plane on a large scale. KOH, HNO₃, and others are commonly used to prepare porous graphene. Zhu *et al.* reported simple activations with KOH to generate nanoscale pores on the exfoliated GO nanosheets^[63]. The result in highly conductive, free-standing, and flexible porous GO paper possessed a very high specific surface area with excellent electrical conductivity and yielded outstanding performance, making it ideal for high-power energy storage^[61,63,64]. Zhao *et al.* introduced carbon vacancy pores into graphene nanosheets using a facile solution method that the HNO₃ reacted with the coordinatively unsaturated carbon atoms to partial detachment and removal of carbon atoms from the nanosheet^[65]. Wang *et al.* prepared porous graphene nanosheets by refluxing reduced GO (rGO) nanosheets in a concentrated HNO₃ solution^[66]. The diameters of nanopores can be readily modulated from several to hundreds of nanometers by varying the acid treatment time^[66]. Besides, H₂O₂^[67] and metal oxides^[68] can also be applied as chemical reagents to etch graphene.

In addition to graphene, other porous 2D nanosheets, such as h-BN^[69], MoS₂^[70,71], and g-C₃N₄^[19], can be obtained through artificial perforation approaches. The atomically thin 2D nanosheets hosting either intrinsic or artificial nanopores impart outstanding molecular transporting and sieving capabilities, making them promising materials for the direct fabrication of selectively permeable membranes with abundant nanofluidic channels.

Nanochannel membrane assembly strategies

In-plane parallel capillaries^[72] are another type of nanochannels that can be constructed by assembling isolated atomic planes of 2D nanosheets into van der Waals heterostructures made layer by layer in a precisely chosen sequence, namely van der Waals assembly [Figure 5A]. A typical stacking procedure starts by isolating micrometer-sized 2D nanosheets on top of a thin supporting film as one brick for the Lego wall, which are then put face-down onto a chosen target with the supporting film removed or dissolved. This process is repeated until the desired stack is assembled. While covalent solid bonds provide in-plane stability of 2D nanosheets, relatively weak, van der Waals-like forces are sufficient to keep the stack together. Radha has made outstanding contributions to this technique, having fabricated narrow and smooth capillaries through van der Waals assembly, with atomically flat graphene sheets at the top and bottom separated by spacers with a precisely controlled number of layers^[73]. They found that the water transport through the channels created by this method was characterized by an exceptionally fast flow that can be attributed to high capillary pressures and large slip lengths and can be associated with the structural ordering degree of nanoconfined water. They also investigated hydrated ion transport through ultimately narrow slits with dimensions approaching the size of small ions and water molecules^[74]. The ions with hydrated diameters larger than the slit size can still permeate through by distortions of their hydration shells. The mobility of ions under angstrom-scale confinement showed a notable dependence on the electric charges inside channels or at their entries. Using the same method, 2D channels made from graphene, MXene, and h-BN allowed helium gas flow that is orders of magnitude faster than expected from theory, whereas similar 2D channels made from MoS₂ exhibited much slower permeation that remains well described by Knudsen diffusion^[75]. It demonstrated the ballistic molecular transport effect that surface scattering could be either diffuse or specular, dependent on the fine details of the atomic landscape of the surface. The van der Waals assembly technique opens up an avenue to making capillaries with channel sizes tunable to angstrom precision and controllable transport properties through a wide choice of available 2D materials as channel walls. These series of 2D nanochannels in the forms of in-plane parallel capillaries provide an ideal experimental platform for offering a new understanding of many excellent nanofluidic observations, such as the unexpectedly high transport of thermal protons^[76,77], the qualitatively different coordination of square ice^[78], the anomalously low dielectric constant of confined water^[79], and the transistor-like electrohydrodynamic effect of hydrated ions^[80].

The assembly of uniform 2D layered films from well-dispersed 2D nanosheets provides an ideal platform for constructing densely packed nanochannels for nanofluidic transport due to the large aspect ratio with atomic thickness and micron lateral dimension. Furthermore, the spaces, including in-plane slits (or defects) and plane-to-plane interlayer galleries within the 2D laminates, create numerous channels for nanofluidic transport. Among various feasible strategies, solution-assisted assembly offers a general, facile, and scalable way for high-throughput constructing densely packed nanochannels from 2D materials. The internal forces, such as electrostatic and van der Waals attractive interactions that are existed inside the 2D laminate, together with external forces, such as compressive, centrifugal, and shear forces that are applied outside the 2D laminate, are largely responsible for tuning the 2D building blocks into the ordered 2D laminar membranes^[81]. Predominantly used solution-assisted assembly methods include pressure/vacuum filtrating, coating, and layer-by-layer assembling.

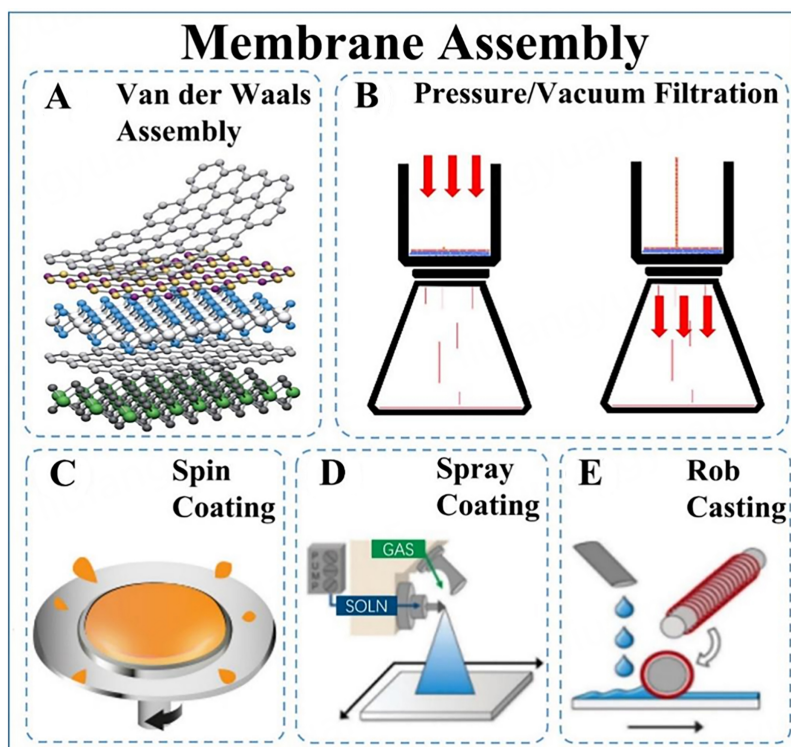


Figure 5. Schematics of the main assembly methods for 2D-material-based nanochannel membranes. (A) Building van der Waals heterostructures^[72]. Copyright 2013, Springer Nature Limited. (B) Pressure/Vacuum filtration. (C) Spin-coating. (D) Spray coating^[181]. Copyright 2011, Royal Society of Chemistry. (E) Rob casting^[181]. Copyright 2011, Royal Society of Chemistry.

The pressure/vacuum filtrating method [Figure 5B] is the most widely adopted to stack 2D laminar membranes. The thicknesses of the membrane can be straightforwardly controlled by altering the loading amount of 2D nanosheets via pressure control. For instance, Dikin *et al.* first reported the preparation of a free-standing GO membrane with macroscopic flexibility and stiffness by vacuum filtration of colloidal dispersions of individual GO nanosheets^[82]. The X-ray spectrum of a typical GO membrane showed a peak corresponding to a layer-to-layer distance (d -spacing) of about 0.83 nm, which can be attributed to an approximately one molecule-thick layer of water that is presumably hydrogen-bonded between the interlocked GO nanosheets within the laminates. Preparation parameters such as driving force, deposition rate, and substrate effect play critical roles in determining the structural formation of 2D laminar membranes. For example, Tsou *et al.* induced the assembly of GO membranes with different laminar microstructures ranging from highly ordered to highly random utilizing pressure, vacuum, and evaporation filtrating techniques^[83].

It is crucial to mention that due to the extremely thin feature, 2D laminates are usually supported by a porous substrate to form practical membranes. The differences in substrate properties also lead to a distinct assembly structure of resulting 2D laminar membranes with uneven performance. An example can be found in the study carried out by Zhang *et al.*, who investigated the effect of substrate on GO membrane formation and separation^[84]. The surface morphology and chemical structure of substrates induced the assembly of GO and determined its adhesion. Furthermore, the bulk pore structure of substrates dominated the whole transport resistance of the GO membrane.

Besides filtrating, various coating methods, such as spin-coating, spray-coating, and casting, have been reported to assemble 2D laminar membranes. During the spin-coating process [Figure 5C], a solution containing 2D materials to be deposited is spread out uniformly over the substrate under centrifugal force, forming the ultrathin and laminar membranes. Kim *et al.* demonstrated two different spin-coating methods to prepare GO membranes on polymeric substrates^[85]. When contacting the substrate surface to the air-liquid interface of the GO solution followed by spin-coating, the repulsive edge-to-edge electrostatic interactions lead to an island-like assembly of GO nanosheets, resulting in a relatively heterogeneous GO stacking structure. In contrast, when contacting the substrate surface to GO solution only during spin-coating, the face-to-face attractive capillary forces created by the spin-coating overcome the repulsive interactions between GO edges, leading to a considerably dense GO laminar deposition. Chi *et al.* found that a speed balance between deposition and solvent (water) evaporation is crucial to obtain smooth GO membranes with uniformly aligned GO nanosheets via spin coating^[86]. Faster deposition may lead to overflow of the solution, while more rapid evaporation will cause uneven distribution of nanosheets. By matching up deposition and evaporation speeds, they obtained a uniform ultrathin GO membrane with a thickness of 20 nm that grants high gas fluxes for efficient gas separation. For spray-coating [Figure 5D], Guan *et al.* carefully controlled spraying times and evaporating rates to achieve facile structure manipulation of GO membrane from disordered-to-ordered and porous-to-compact^[87]. Ibrahim *et al.* further verified that using dilute concentration GO suspensions in spray-coating can help minimize the edge-to-edge interactions and reduce extrinsic wrinkles formation^[88]. Casting [Figure 5E] also belongs to coating methods that allow the continuous production of large-scale membranes. Akbari *et al.* utilized the flow properties of a nematic GO fluid in developing an industrially adaptable process to produce GO membranes with large in-plane order and stacking periodicity by shear-induced alignment of liquid crystals of GO^[89]. Zhong *et al.* showcased a universal, scalable, efficient continuous centrifugal casting method to produce highly aligned and compact 2D laminar membranes with impressive performances^[90]. Fluid mechanics analyses indicated that the simultaneous generation of shear force and centrifugal force during the continuous centrifugal casting process could be responsible for the alignment and compaction of 2D nanosheets, respectively.

Layer-by-layer assembly is a flexible construction process involving alternate deposition of different materials, often using one or more of the previously described methods. Such a flexible layer-by-layer construction process enables precise control over the thickness of the selective layer by varying the number of deposition cycles and is beneficial for introducing various interlayer stabilizing forces, including covalent, electrostatic, or hydrogen bindings between adjacent 2D nanosheets, thereby producing membranes with robust and ordered laminar structures^[81]. Hu *et al.* reported a 1,3,5-benzenetricarbonyl trichloride cross-linked GO membrane made via layer-by-layer deposition^[91]. The covalent cross-linking enhanced the stability of the stacked GO nanosheets, overcoming their inherent dispensability in the water environment while fine-tuning their charges, functionality, and spacing^[91]. In addition, layer-by-layer assembly has been used to create stable GO membranes through the electrostatic bonding of negatively charged GO nanosheets and positively charged polyallylamine hydrochloride^[92]. These methods provide a gateway to rationally design the charge properties and other functionalities of interlayer nanochannels of 2D laminar membranes by carefully choosing the intercalated molecules, polyelectrolytes, or nanomaterials. For instance, Song *et al.* developed both positively charged polyallylamine hydrochloride@GO and negatively charged polystyrene sulfonate@GO, which they alternately deposited on polycarbonate substrates by the layer-by-layer assembly, producing polyelectrolyte intercalated GO membranes with tunable charge-gating ion exclusion effects^[93]. Apart from a single interaction, Zhao *et al.* fabricated GO-based hybrid membranes via layer-by-layer self-assembly of gelatin molecules and GO nanosheets driven by multiple interactions, including electrostatic attraction, hydrogen bond, and hydrophobic interaction^[94]. Electrostatic attractions were formed between ionized carboxyl groups on GO and protonated amino groups on gelatin, hydrogen

bonds between various polar groups on gelatin and GO, and hydrophobic interactions between the hydrophobic carbon backbone of GO and hydrophobic amino acid side chains on gelatin. These multiple interactions may contribute to the formation of highly ordered 2D laminar membranes with finely tuned 2D nanochannels for nanofluidic transport.

In summary, the structural properties of nanochannels in nanochannel films based on 2D materials, including layer thickness, stacking order, defects and grain boundaries, surface functionalization, embedding of additives or polymers, and nanosheet alignment and orientation, largely affect the overall filtration performance of the membrane. Controlling these factors can tune the interlayer spacing, pore size distribution, surface interactions, and flow dynamics within nanochannels, leading to membranes with higher selectivity, permeability, and fouling resistance. The choice of synthesis and assembly method depends on the desired material, application, scalability, and desired quality of 2D nanosheets. Each method has its advantages and limitations. Further studies to understand and optimize these structural properties will facilitate the development of more efficient and tailored nanochannel membranes for various separation applications.

Characterization methods

Characterization techniques are essential for understanding the properties of 2D materials. Various techniques allow for a thorough examination of these materials. XRD is used to determine the crystal structure and orientation of 2D materials. It involves directing X-rays onto the material and measuring the resulting diffraction pattern. XRD can provide information about lattice parameters, crystal symmetry, and the presence of specific crystalline phases. In addition, the layer spacing is calculated using XRD data according to Bragg's law. Optical spectroscopy techniques such as UV-Vis absorption spectroscopy and photoluminescence spectroscopy are used to study the optical properties of 2D materials. They can reveal information about the material band gap, exciton properties, and light-matter interactions. X-ray photoelectron spectroscopy (XPS) is used to analyze the chemical composition and electronic states of 2D materials. It involves irradiating the surface of a material with X-rays and measuring the energy of the emitted electrons. XPS can provide information about elemental composition, chemical bonding, and the presence of impurities or functional groups. Raman spectroscopy is used to analyze the vibrational modes of 2D materials. It involves shining a laser on the material and measuring the scattering spectrum. Raman spectroscopy provides insight into the crystal structure, composition, and strain of material and identifies different types of 2D materials. Atomic Force Microscopy (AFM) is a powerful technique for imaging the morphology and surface properties of 2D materials. It uses a sharp probe to scan the entire surface of a material, detecting force changes between the probe and the sample. AFM can provide information about the height, roughness, and mechanical properties of a material at high spatial resolution. Scanning electron microscopy (SEM) provides high-resolution images of the surface/sectional morphology of 2D materials. It uses a focused electron beam to scan the surface of a material, generating detailed images that reveal features such as the size, shape, and arrangement of thin sheets or layers of material. Transmission electron microscopy (TEM) is used to study the internal structure and atomic-level features of 2D materials. It involves the transmission of an electron beam through a thin sample to image the atomic structure and defects of the material. TEM can provide information about crystal structure, grain boundaries, stacking sequences, and even individual atomic arrangements.

Among other things, these characterization techniques allow researchers to gain a comprehensive understanding of the structural, morphological, chemical, and optical properties of 2D materials. By combining multiple techniques, a complete characterization of 2D materials can be achieved, facilitating their optimization and utilization in a variety of applications. The development of advanced characterization techniques, such as cryoelectron microscopy and *in-situ* Raman, will provide researchers

with more reliable means and opportunities to explore the deeper mechanisms of structure and separation and purification of 2D-material-based membranes^[95-98].

REGULATING NANOCHANNELS

The transport of nanofluids through nanochannel membranes based on 2D materials predominantly takes place within the interlayer space. It is within this space that the transport behavior is influenced by various physical and chemical factors. Moreover, addressing issues such as nanochannel instability, instability at the 2D-material interface, and swelling can be effectively tackled by adjusting the physicochemical factors of the 2D-material-based nanochannels. Therefore, rational regulation of the nanochannels is of utmost importance. Controlling the physical factors of channel size, channel length, and channel morphology can primarily modulate nanofluidic transport by achieving precise sieving, shortening the transport distance, and reducing the transport resistance. Regulating the chemical factors of the surface chemistry effects can specifically facilitate nanofluidic transport through various permeant-channel interactions. Many efforts have been devoted to carefully designing precise geometries and favorable chemical features of nanochannels for realizing fast and selective molecular/ionic transportation. This section presents typical provisions for the physicochemical properties of nanochannels in 2D-material-based membranes. Based on experimental and theoretical studies, various effects and in-depth structure-property relationships of nanofluid transport are also discussed.

Regulating size of nanochannels

In 2D-material-based nanochannel membranes, nanofluidic transport occurs in interlayer capillaries and wrinkles formed by adjacent 2D nanosheets and inter-edge gaps and intrinsic pores formed on planar 2D nanosheets interconnect with each other to create numerous nanochannels. Firstly, the channel size [Figure 6], one of the most prominent characteristics of nanochannels, firmly decides the entry of nanofluids. Joshi *et al.* found that the interlayer spacing of a GO membrane was ~ 0.9 nm^[16], allowing any ion or molecule with a hydrated radius of 0.45 nm or less to enter the nanochannels and permeate at a speed order of magnitude faster than would occur through simple diffusion, while all species larger than this are sieved out. Such sharp size cutoff determined by the interlayer spacing has significant implications on a myriad of occasions. By adjusting the channel size through diverse methods, such as confinement, reduction, cross-linking, and intercalation, a broad range of different-sized nanochannels can be designed to sieve target ions and molecules from the bulk solution precisely.

Due to the inevitable swelling effect when immersed, hydration would increase the size of nanochannels and deprive their sieving capability. Achieving a small channel size for the 2D laminates immersed in solvents has been a challenging task. Abraham *et al.* described a physical confinement method [Figure 6A] to control the interlayer spacing from ~ 9.8 Å to ~ 6.4 Å to obtain accurate and tunable ion sieving^[99]. GO laminates were stored at different relative humidities to yield controllable interlayer spacing attributed to incorporating water molecules into various sites between GO nanosheets. Subsequently, epoxy was used to encapsulate stacked GO laminates for preparing physically confined GO membranes since the epoxy mechanically restricts laminate swelling upon water exposure. As ions and water permeate along the GO nanochannel, the permeation rate for Na⁺ and K⁺ showed an exponential dependence, decreasing by two orders of magnitude as interlayer spacing decreased from 9.8 Å to 7.4 Å. However, the water permeation rate showed only a slight variation, reducing by a factor of ~ 2 within the same range of interlayer spacing. The former is related to the partial clogging of graphene capillaries, and the latter is attributed to a low barrier and a large slip length for water in graphene capillaries. Similarly, Li *et al.* reported an external pressure regulation method for controlling the interlayer spacing of GO laminates against swelling^[100].

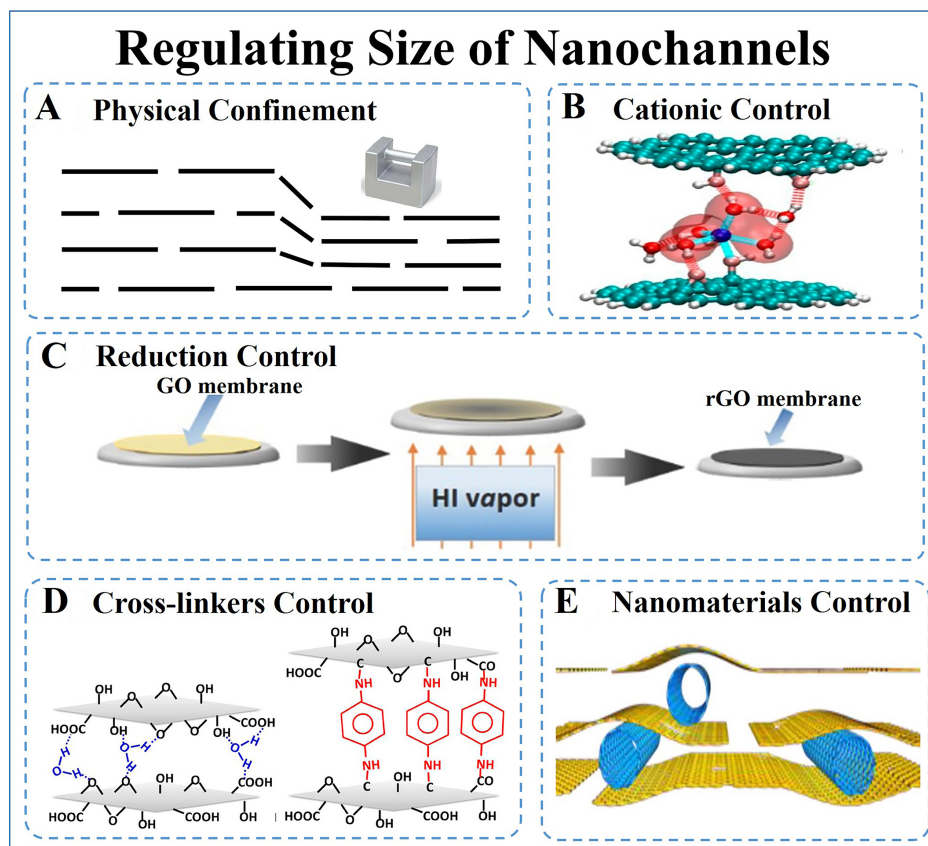


Figure 6. Regulating the size of nanochannels. (A) Physical confinement. (B) The stable, optimized geometries of $\text{Na}^+(\text{H}_2\text{O})_6$ @GO clusters from density functional theory computation^[101]. Copyright 2017, Springer Nature. (C) The fabrication procedure of free-standing rGO membranes using reduction control^[104]. Copyright 2015, John Wiley & Sons, Inc. (D) Original GO membrane (left) and the composite GO-framework prepared by *p*-phenylenediamine cross-linking GO membrane (right)^[105]. Copyright 2014, American Chemical Society. (E) Graphene/carbon nanotube composite membranes are prepared by assembling refluxed GO (rGO) and multi-walled carbon nanotubes^[120]. Copyright 2015, American Chemical Society.

Apart from channel size regulation based on external forces, cationic control is a representative method of channel size regulation based on internal forces. Chen *et al.* demonstrated cationic control of the interlayer spacing of GO membranes with angstrom precision using K^+ , Na^+ , Li^+ , Ca^{2+} , or Mg^{2+} ions [Figure 6B]^[101]. The confinement of interlayer spacing is mainly due to the interaction between hydrated cations and aromatic rings (cation- π interactions) on the GO nanosheet and the interaction between hydrated cations and the oxygenated groups on the GO nanosheet. As a result, the interlayer spacing controlled by one type of cation can efficiently and selectively exclude other cations with larger hydrated volumes. Especially the K^+ -controlled GO membranes can even reject K^+ itself owing to the comparable interaction energy between K^+ and GO nanosheets concerning the dehydration energy of K^+ .

Reduction is another effective method to control the small channel size for the solvated 2D laminates. These 2D nanosheets possess abundant functional oxygenated groups that open the interlayer spacing between adjacent nanosheets and allow solvent molecules to intercalate into 2D laminates. Partially removing these oxygenated functional groups through various thermal or chemical reductions can enhance interlayer π - π interactions, thereby producing narrowed and stabilized nanochannels. Qiu *et al.* reported that hydrothermal treatment could readily control the reduction of GO nanosheets in water^[102]. Meanwhile, Han *et al.* obtained an rGO dispersion by base-refluxing to generate moderate holes and create a large number of

permeation “gates”, ultimately increasing the permeability of the rGO membrane^[103]. However, the pre-treatment of reduction may lead to the worse dispersion of nanosheets that is not conducive to uniformly assembling them into well-stacked laminates. Liu *et al.* prepared a GO membrane beforehand and placed it above a hydrogen iodide (HI) solution [Figure 6C]^[104]. The HI steam acts as a reducing agent, which reduces GO and triggers the initial delamination between the rGO membrane and substrate. Fumagalli *et al.* found that GO laminates reduced using thermal, HI, and VC reductions are highly impermeable to strong chemicals and salt solutions, owing to a high degree of graphitization of the laminates, causing nanochannels collapse during the reduction process^[79].

The enlarged channel size can be achieved by cross-linking or intercalating cross-linkers, such as specific molecules, polyelectrolytes, or nanomaterials, to reinforce transport efficiency. The most commonly used cross-linkers for GO membranes are diamines^[105], including ethylenediamine (EDA), butylenediamine (BDA), and phenylenediamine (PDA), which can chemically bond with adjacent GO nanosheets through condensation and nucleophilic addition reactions [Figure 6D]. The spatial configuration of amine monomers primarily determines the channel size of cross-linked GO membranes in a dry state, whereas the bonding strength of amine monomers within the GO laminate likely determines their channel size in a wet state^[106]. Other molecules holding characteristic terminal groups, such as dicarboxylic acids^[107], tannic acid^[108], borate^[109], isophorone diisocyanate^[110], porphyrins^[111], and polybenzimidazole^[112], have also been proved to cross-link 2D-material membranes to address 2D channel size control chemically. Yang *et al.* demonstrated the preparation of thiourea covalently linked GO membrane where thiourea bridged GO laminates periodically through the reactions of amino and thiocarbonyl groups with the functional groups of GO, leading to mechanically stable and structurally well-defined 2D channels^[113]. These molecule cross-linkers usually yield covalent bonds through a limited number of active sites. In contrast, polyelectrolytes possess long polymer chains with abundant functional groups, which can serve as polymer cross-linkers to be incorporated into 2D laminates through sufficient active sites to produce a dense composite structure. The commonly used polymer cross-linkers are polyvinyl amine (PEI)^[114,115], polyvinyl alcohol (PVA)^[116], polyethylene glycol (PEG)^[117], and so on. Ran *et al.* utilized imidazolium-functionalized brominated poly (2,6-dimethyl-1,4-phenylene oxide) (Im-PPO) and sulfonated poly (2,6-dimethyl-1,4-phenylene oxide) (S-PPO) to connect neighboring GO nanosheets via non-covalent π - π , electrostatic, and hydrogen bonding interactions^[118]. These cross-linking strategies may pave the way to access highly stable and efficient transport of 2D lamellar membranes.

Besides cross-linking, intercalating nanomaterials of specific sizes is another means to significantly improve the permeability of 2D-material membranes, as it effectively creates large amounts of broadened pathways for nanofluidic transport. Carbon-based nanomaterials, metal oxide nanoparticles, MOFs, and COFs are among the representative intercalated nanomaterials. By embedding carbon nanodots of controllable sizes, Wang *et al.* were able to tune the permeability of GO membranes^[119]. Han *et al.* expanded the interlayer spacing of GO membranes by intercalating multi-walled carbon nanotubes (CNTs) [Figure 6E]^[120]. Goh *et al.* further proposed that intercalating of CNTs of different diameters can effectively inhibit the restacking (or aggregation) of GO nanosheets and thus create plenty of nanochannels for water transport while retaining the molecular sieving capability of the ensuing membranes. Moreover, CNTs can also act as anchors to interact and interconnect with the adjacent GO nanosheets due to the perfect compatibility of carbon-based materials to reinforce the membrane stability^[121]. Intercalation of metal oxide nanoparticles is another general and scalable approach to expand 2D nanochannels significantly. Zhang *et al.* prepared nanoparticles@GO membranes using a simple *in-situ* solvothermal synthesis method, where size- and density-controllable nanoparticles were uniformly grown on GO nanosheets through coordination^[122]. Compared to the membrane produced by filtering GO solutions mixed directly with nanoparticles, the *in-*

situ fabricated nanoparticles@GO membrane uniformly introduced nanoparticles within GO laminates without damaging their initial ordered stacking structures and hence exhibited ultrahigh water permeance and excellent rejections for various solutes in water, as well as good stability under high pressure and cross-flow operation. This general concept of intercalation can also be demonstrated by several kinds of nanoparticles such as TiO₂^[123], silica^[124], and hydroxy sodalite nanocrystals^[125], endowing nanoparticles intercalated GO membranes with additional multifunctions. Compared with nonporous metal oxide nanoparticles, intrinsically porous nanocrystals are more beneficial for fast nanofluidic transport when they are intercalated into 2D nanochannels. By incorporating MOFs^[126,127], COFs^[128,129], and biomimetic water channels^[130] with extra internal pathways through sub-nano-sized apertures as the microporous fillers into 2D laminates, both the size and the number of nanochannels are increased, leading to greatly enhanced nanofluidic transport performance. Li *et al.* described a route for fabricating MOFs channeled graphene composite membranes with molecular sieving properties using *in-situ* crystallization. A series of MOFs, including ZIF-8, ZIF-7, CuBTC, and MIL-100, were showcased to be impregnated into interlayers of GO laminates, which firmly anchored and bolstered up GO laminates by coordination bonds to form a highly porous architecture with uniform nanochannels^[127].

Khan *et al.* created a hybrid laminar membrane by assembling COFs and GO nanosheets^[128]. The incorporation of COFs nanosheets provides a large number of pores that shorten the transport pathway while retaining the interlayer distance. Similarly, Sui *et al.* also intercalated rigid 2D COFs into GO laminates to realize a robust GO/COF laminar membrane^[129]. The atomically thin 2D COFs with pores serve as a nano spacer to increase the interlayer spacing between GO nanosheets and provide direct transfer channels, thereby reducing water transfer resistance. On the other hand, the COFs enhance the self-supporting capacity of GO networks on a substrate with large pores. As a result, this strategy led to a significant increase in the water permeance of the optimized GO/COF laminate membrane compared to the pristine GO membrane without compromising its rejection rates to organic dyes. Mao *et al.* embedded imidazole-ureido bola-amphiphile-imidazole compound as biomimetic imidazole-quartet water channels into assembled GO laminates to enhance water transport selectivity over butanol benefiting from the hydrophilic water-preferential nanochannels along the imidazole-ureido molecular scaffolds^[130].

As the GO membrane is a showpiece that provides flexible platforms for developing versatile novel 2D-material membranes, the methods mentioned above for regulating channel size are adaptable for other 2D-material membranes. For example, Wang *et al.* related the performance of MoS₂ membranes to the size of their nanochannels in different hydration states^[131]. They found that the water-impermeable behavior of the dry MoS₂ nanochannel, which has a 0.62 nm interlayer spacing, is caused by the irreversible nanosheet restacking during a drying process. In comparison, the fully hydrated MoS₂ membrane possesses a stable 1.2 nm interlayer spacing, leading to high water permeability and moderate-to-high ionic and molecular rejection. Meanwhile, the MoS₂ nanochannel has a much stronger van der Waals attraction force than the GO nanochannel, which prevents the interlayer spacing from increasing, thereby ensuring the aqueous stability of MoS₂ membranes. Inspired by the structural characteristics of GO membranes, where oxidized zones act as spacers to provide a relatively large interlayer distance to accommodate water molecules, Ran *et al.* incorporated appropriate acid spacers between g-C₃N₄ interlayers to enlarge the width of the 2D channels^[132]. The intercalation molecules successfully break up the tightly stacked structure of g-C₃N₄ laminates. Accordingly, the modified g-C₃N₄ membranes give rise to two orders of magnitude higher water permeance without sacrificing the separation efficiency. In a similar route, Wang *et al.* devised a method to partially exfoliate dg-C₃N₄ nanosheets with artificial nanopores and unstripped fragments as self-supporting spacers and assemble them into 2D laminar membranes for water purification^[13]. The artificial nanopores and the spacers between the partially exfoliated g-C₃N₄ nanosheets provide numerous nanochannels for

nanofluidic transport with ultralow friction while effectively retaining larger molecules. Wang *et al.* also demonstrated a strategy for stabilizing the $Ti_3C_2T_x$ laminar architecture by alginate hydrogel pillars formed between the adjacent nanosheets^[133]. After pillared by different alginate hydrogel pillars, the nanochannel diameters are effectively fixed at ~ 7.4 Å, and the resulting membrane exhibited significantly enhanced the ion-sieving property with distinct ions permeation cutoff depending on the multivalent cations cross-linked with alginate molecules.

Regulating the length of nanochannels

Another physical factor influencing nanofluidic transport through 2D-material-based nanochannel membranes is channel length, which largely depends on the membrane thickness and porosity. Nanoporous 2D materials of single- or few-atom thickness are the ultimate building blocks for constructing ultrathin membranes with minimal resistance to maximize permeance.

As a straightforward way to shorten the channel length, many theoretical and experimental studies have demonstrated the ultrafast permeation performance of ultrathin 2D-material membranes. For example, Cohen-Tanugi *et al.* predicted that ultrathin nanoporous graphene membrane could have water permeability several orders of magnitude higher than conventional membranes thanks to the chemical functionalization, which may have a valuable role to play in water purification [Figure 7A]^[134]. Han *et al.* fabricated ultrathin (~ 22 -53 nm) graphene nanofiltration membranes on microporous substrates for efficient water purification^[103]. Liu *et al.* prepared free-standing ultrathin rGO membranes with thickness down to ~ 20 nm by HI vapor and water-assisted delamination^[104]. Yang *et al.* reported highly laminated GO membranes of only several layers in thickness (~ 8 nm), exhibiting outstanding sieving properties accompanied by ultrafast solvent permeation^[135]. Li *et al.* described a reproducible facile filtration method to produce ultrathin GO membranes down to 1.8 nm in thickness, which exhibited superior gas separation performance^[136]. Furthermore, single-layer 2D-material membranes for practical use have also been attempted. For example, Heiranian *et al.* showed that a single-layer nanoporous MoS_2 effectively allowed water transport at a high rate associated with permeation coefficients, energy barriers, water density, and velocity distributions in the pores [Figure 7B]^[137].

Although the ultrathin 2D-material membranes exhibit exceptional permeation performances, the limited mechanical strength of these membranes over large areas remains a hindrance to their widespread use. To overcome this limitation, Yang *et al.* reported the production of an atomically thin nanoporous membrane with a single-layer graphene nanomesh (GNM) supported by an interwoven network of single-walled carbon nanotubes (SWNT)^[138]. The monolayer GNM featuring high-density subnanometer pores [Figure 7C] allows efficient transport of water molecules with minimum resistance while effectively blocking solute ions or molecules to enable size-selective separation. The mechanically strong, interconnected SWNT network, acting as the microscopic framework, separates the GNM into micro-sized islands, thus ensuring the structural integrity of the atomically thin GNM. The resulting large-area, ultrathin GNM/SWNT hybrid membrane showed high water permeance and excellent size selectivity combined with excellent anti-fouling characteristics, making it highly attractive for energy-efficient and robust water treatment.

Regulating morphology of nanochannels

The morphology of the channel in ultrathin 2D-material membranes plays a crucial role in determining the distance traveled by nanofluids. Inter-edge gaps [Figure 8A] and intrinsic pores [Figure 8B] are crucial elements that influence this distance^[135,136]. Ibrahim *et al.* proposed using nanofluidic pathways in laminar GO membranes, where permeation occurs through pinholes within GO flakes and capillaries between them^[139]. Utilizing small and porous nanosheets to assemble membranes can efficiently introduce more

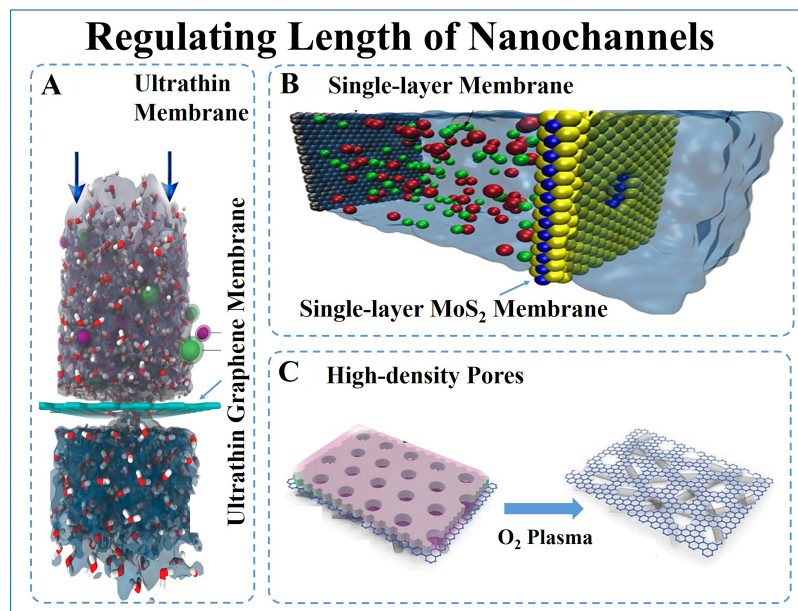


Figure 7. Regulating length of nanochannels. (A) side view of the computational system of ultrathin graphene membrane in the desalination process^[134]. Copyright 2012, American Chemical Society. (B) The simulation box consists of a single-layer MoS₂ sheet (molybdenum in blue and sulfur in yellow), water (transparent blue), ions (in red and green), and a graphene sheet (in gray)^[137]. Copyright 2015, Springer Nature. (C) The fabrication process of density pores on graphene-nanomesh/carbon-nanotube hybrid membranes using O₂ plasma^[138]. Copyright 2019, Science Publishing Group.

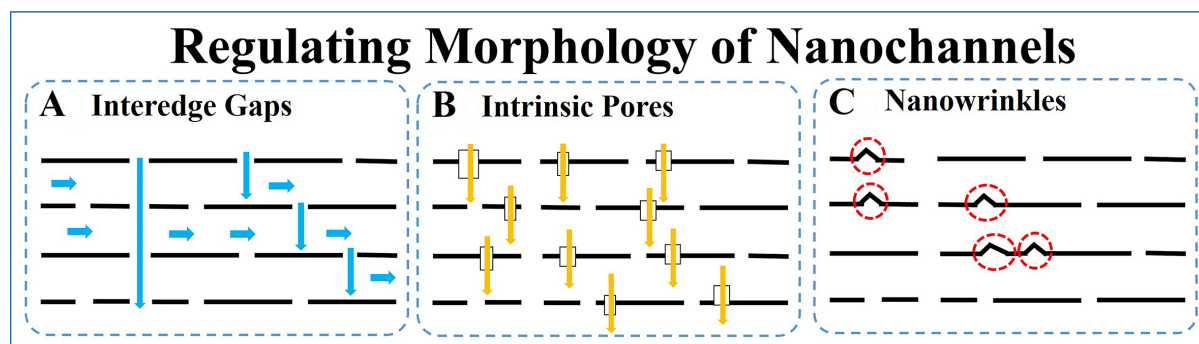


Figure 8. Regulating morphology of nanochannels: inter-edge gaps (A), intrinsic pores (B), and nanowrinkles (C).

inter-edge gaps and intrinsic pores, enabling nanofluids to take shortcuts to perform ultrafast transport. A few works have developed simple methods for the lateral size fractionation of 2D nanosheets using techniques such as sonication^[140], filtrations^[141], differential centrifugation^[142], and controlled directional freezing^[143]. It is found that when the dimension of nanosheets within the membrane is changed from microsize to nanosize, the amount of nanofluidic pathways formed within the GO membrane is increased significantly, resulting in the enhancement of trans-membrane transportation in the case of nanosized 2D-material membranes^[144]. Nie *et al.* exploited this concept of lateral dimension control to engineer shorter and less tortuous transport pathways for solvent molecules, leading to the development of small-flake GO membranes that achieved ultrafast selective molecular transport^[145]. The methanol permeance in these membranes reached up to 2.9-fold higher than its large-flake GO counterpart, with high selectivity towards organic dyes^[145]. Section 2.2 has described various perforation techniques to produce nanopores on 2D

nanosheets^[15,19,58-71]. The creation of nanopores can provide a greater number of transport nanochannels for nanofluids and sharply reduce the average transport distances. Ying *et al.* reported GO membranes with introduced in-plane mesopores by a reoxidation process, demonstrating 2-3 folds enhancement of water permeance as that of the pristine GO membranes^[146]. Li *et al.* also proposed thermally reduced nanoporous GO membranes through a combination of mild H₂O₂ oxidation and moderate thermal treatment, increasing the water permeability by 26 times^[147]. Those intrinsically porous 2D materials are more attractive as building blocks to assemble 2D laminar membranes. Their uniform nanopores consisting of angstrom-sized windows and nanometer-sized cavities can provide numerous cross-layer shortcuts and ensure precise size exclusions. Peng *et al.* reported ultra-permeable and super selective molecular sieve membranes made of 2D MOF nanosheets, which achieved H₂ permeance of up to several thousand GPU with H₂/CO₂ selectivity greater than 200^[37,148]. Shinde *et al.* demonstrated ultrathin 2D COF membranes with a well-defined ordered porous structure^[149]. These membranes displayed remarkable permeabilities for polar and nonpolar organic solvents, which were approximately 100 times higher than the amorphous polymer membranes^[149].

Besides the tortuous transport pathways through internal nanochannels of 2D laminar membranes extending in horizontal and vertical directions, nanowrinkled morphologies [Figure 8C] also exist in 2D laminar membranes, whose effects in transmembrane transport should not be neglected. Xi *et al.* proposed an rGO membrane with 2D nanochannels uniformly confined with a space size of $\sim 8 \text{ \AA}$ ^[150]. The mild reduction avoids the hydrothermal corrugation of GO nanosheets and thus enables the creation of highly parallel 2D nanochannels for precise sieving of mono-/multi-valent metal ions^[150]. Li *et al.* also demonstrated a mild-thermal annealing for preparing rGO membrane for nanofiltration since the mild reduction condition might favor the formation of a more ordered and better-controlled transport nanochannel^[151]. Contrary to these efforts to eliminate nanowrinkles, Saraswat *et al.* hypothesized that the imperfect stacking in the 2D laminates could lead to voids, wrinkles, and disordered microstructures that could provide alternative non-ideal transport pathways for nanofluids, resulting in a higher effective permeance^[152]. Kang *et al.* further revealed the roles of nanowrinkles in mass transport across GO membranes^[153]. They found nanowrinkles by themselves serve as fast transporting ways while their connection with narrow interlayer channels can form a selective network^[153]. Huang *et al.* developed a nanostrand-channeled GO membrane, whose permeance offered a 10-fold enhancement without sacrificing the rejection rate compared with that of pristine GO membrane, attributing to the generation of more nanofluidic channel networks in the membrane^[154]. The nanostrand-channeled concept is also extendable to other 2D laminar membranes, such as MXene^[17] and WS₂ membranes^[155], for increased permeability. These findings corroborate that nanowrinkles serve as fast tracks for nanofluids to enhance membrane permeability. Considering nanowrinkles broadly existing within flexible 2D nanosheets, they are expected to show critical transportcontrolling effects in nanofluidic transport in 2D-material membranes.

Regulating surface physicochemical properties of nanochannels

The 2D-material nanosheets have abundant functional groups. During the filtration process, the 2D material-based membrane is prone to swelling effect, resulting in the collapse of nanochannels and loss of sieving performance. Targeted modification of 2D-material surfaces is, therefore, significant, and a number of methods have been developed for modifying the chemical properties of membrane surfaces [Figure 9]. One commonly used strategy is the Chemical intercalation of cross-linking agents (e.g., ions, small molecules, or macromolecules), which enhances the interlayer force and improves the mechanical stability of 2D nanosheet membranes. At the same time, this strategy modulates the affinity of water/ions to the nanosheet surfaces, thereby regulating their mobility as they pass through the channels.

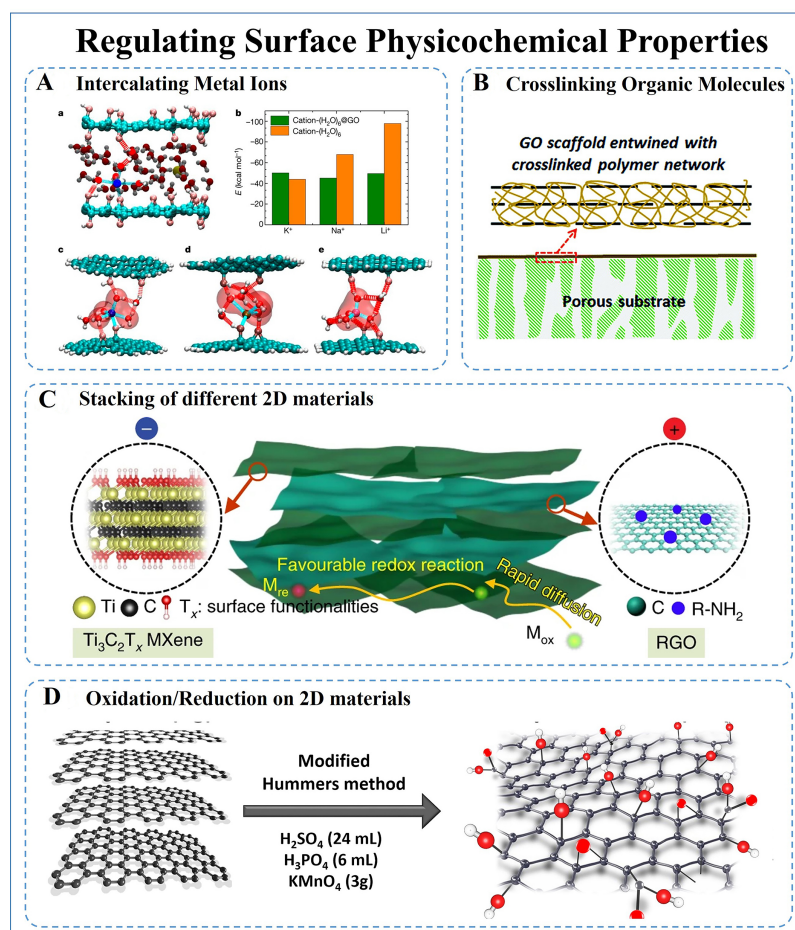


Figure 9. Regulating surface physicochemical properties of nanochannels. (A) Intercalating metal ions. [a] A snapshot of the ab initio molecular dynamics simulation at 27 ps. [b] The interaction energy between hydrated cations and graphene oxide sheets [labeled cation-(H₂O)₆@GO] and the hydration energy of the cation [labeled cation-(H₂O)₆]. [c–e] The most stable optimized geometries of cation-(H₂O)₆@GO clusters from density functional theory computation, where the cations are Na⁺, K⁺, and Li⁺. Copyright 2017, Springer Nature. (B) A GO polymer cross-linked network composite membrane for forward osmosis desalination. Copyright 2017, The Royal Society of Chemistry. (C) Restacked Ti₃C₂T_x-based membrane by introducing reduced GO as the spacer. Copyright 2019, Springer Nature. (D) Oxidation process from graphite to graphene oxide. Copyright 2021, MDPI.

Modifying the surface of 2D materials with a small number of metal ions, such as Mg²⁺ and Ca²⁺, is considered an effective strategy to improve the membrane performance significantly. This enhancement is mainly due to the electrostatic bonding between metal ions and functional groups on the surface of 2D materials^[156]. To further understand this mechanism, Chen *et al.* modified the GO membrane with hydrated Na⁺ ions and found, through DFT calculations, that the hydrated ions were adsorbed through hydrogen bonds in the region where the oxidized groups and aromatic rings coexisted, effectively adjusting and fixing the interlayer distance^[101]. The interlayer distance is proportional to the hydration radius of the corresponding Li⁺ > Na⁺ > K⁺ class ions [Figure 9A]. Ding *et al.* effectively reduced the d-spacing to ~ 1.5 nm. They effectively suppressed the swelling effect by intercalating Al³⁺ into the Ti₃C₂T_x MXene film combined with abundant surface termini (such as ¼O, eOH, and eF functional groups) within the nanosheets^[157]. Cross-linking 2D materials by organic molecules is another effective strategy to tune and fix the interlayer distance in layered films. Epoxy, a commonly used chemical raw material, is employed to modify the surface of 2D-material nanosheets. This strategy successfully prevented the swelling of GO and produced nearly 97% NaCl repulsion^[99]. Hung *et al.* cross-linked GO with EDA monomer to make the

nucleophilic substitution condensation reaction between the oxygen-containing groups of amine and GO to form a CeN covalent bond, which effectively suppressed the swelling effect^[105]. *In-situ* polymerization on the surface of 2D materials to generate twins is also a commonly used strategy^[72-75]. Kim *et al.* using N,N'-methylenebisacrylamide (MBA) as the cross-linking agent, N-isopropylacrylamide (NIPAM) as the monomer, and then ammonium persulfate (APS) as the initiator, successfully synthesized the GO@polymer twins^[158]. The prepared membranes have excellent anti-swelling properties and desalination ability^[158,159] [Figure 9B].

The potential interaction of functional groups on the surfaces of different 2D materials makes the superimposition of different 2D materials a possible strategy for modifying the surface chemistry of materials [Figure 9C]. Xie *et al.* reported a $Ti_3C_2T_x$ MXene-based membrane whose microstructure was optimized by inserting rGO between the layers^[160]. The surface of the membrane was progressively hydroxylated to increase the accessibility of $Ti_3C_2T_x$, thus improving the wettability of the film and enhancing the adsorption and reduction of heavy metal ions.

Oxidation and reduction processes are commonly used to modify and prepare 2D materials, so surface properties are often modified during the preparation process. For example, using a modified Hummers method (i.e., oxidation procedures), Alkhouzaam *et al.*^[161] prepared a GO membrane with more active surface properties than a graphene membrane, which facilitates its functionalization to meet the request [Figure 9D].

The properties of nanochannel membranes based on 2D materials, including swelling resistance and water permeability and retention, are closely related to the transport control effects of nanochannels and the interleaving of surface properties. These factors play a key role in determining the overall performance and functionality of the membranes. Therefore, it becomes imperative to thoroughly evaluate and consider the effects of various modification methods on the nanochannels. This careful evaluation enables researchers to select and optimize the most suitable 2D-material-based membranes for specific applications. By understanding and exploiting the complex relationship between nanochannels and surface properties, researchers can unlock the full potential of these membranes in areas as diverse as water purification to energy storage.

APPLICATIONS OF 2D-MATERIAL-BASED NANOCANNEL MEMBRANES

By rationalizing the structural and functional characteristics, 2D-material-based nanochannel membranes can achieve many features, such as ultrafast transmission, selective sieving, sensitive sensing, controlled gating, and rectification, among others. This section summarizes typical developments in liquid molecular separation, gas separation, and ion sieving using state-of-the-art 2D-material-based nanochannel membranes [Figure 10].

Liquid molecular separation

Membranes are highly susceptible to swelling effects when applied in liquid environments (i.e., liquid molecular separations, including liquid solvent-molecular solute separations and liquid-liquid separations), leading to the collapse of nanochannels, reduced selectivity, and shortened membrane lifespan. Therefore, it is imperative to improve the swelling resistance of membranes in liquid environments compared to membranes in other conditions.

A series of anti-swelling MXene nanochannel membranes were synthesized by Xing *et al.* using the interaction forces generated by introducing negatively charged polymers into positively charged MXene

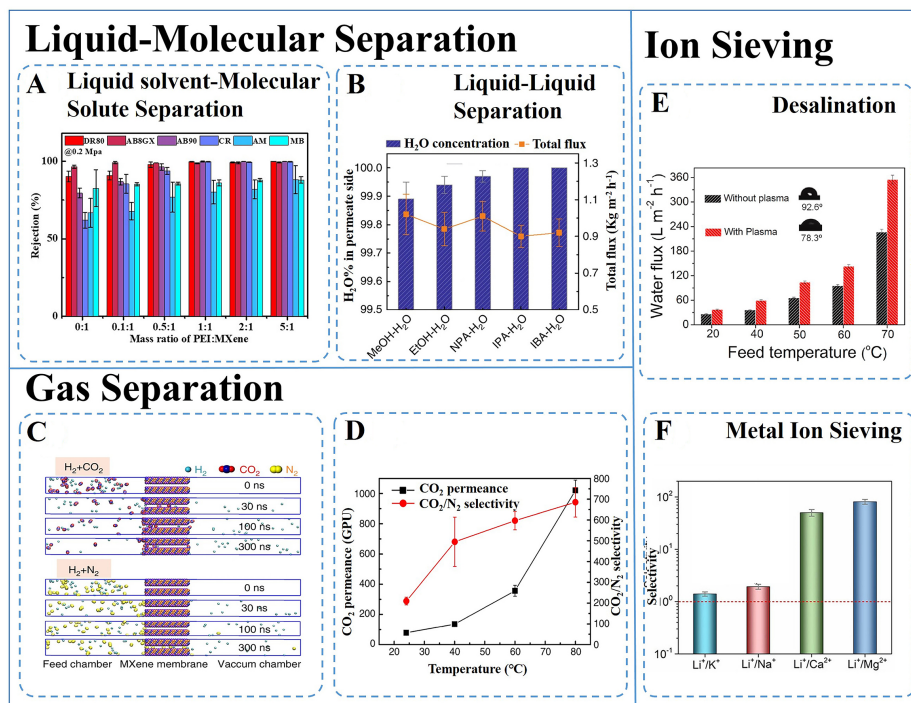


Figure 10. Liquid-molecule separation performance in representative applications. (A) Rejection rates of various dyes (i.e., Liquid solvent-Molecular solute separation) on an anti-swelling MXene-based membrane^[162]. Copyright 2022, John Wiley & Sons, Inc. (B) Separation performance of various alcohols to H₂O (i.e., Liquid-liquid separation) on a 2D-interspacing-narrowed graphene oxide membrane^[163]. Copyright 2017, Springer Nature. Gas separation performance in representative applications. (C) Simulation diagram of highly efficient gas separation on MXene molecular sieving membranes^[164]. Copyright 2018, Springer Nature. (D) Highly efficient CO₂ capture performance on ultrathin graphene oxide-based hollow fiber membranes with brush-like CO₂-philic agent^[165]. Copyright 2017, Springer Nature. Ion sieving performance in representative applications. (E) Ultrafast water flux of a graphene desalination membrane with 99.99% NaCl rejection rate at different feed temperatures^[167]. Copyright 2021, Elsevier B.V. (F) Fast and selective lithium-ion transport performance on an oriented UiO-67 Metal-Organic Framework membrane^[170]. Copyright 2022, John Wiley & Sons, Inc.

membranes^[162]. And by tuning the ratio of polymer and MXene, different sizes of nanochannels can be obtained for separating different hydrated molecules [Figure 10A]. Xing *et al.* reported a separation membrane that can adjust the size of nanochannels by operating pressure, which can retain 99.9% of hydrated dye molecules under a small operating pressure and 51.8% of the hydrated ions under a large operating pressure^[14]. Liquid-liquid separation plays a pivotal role in chemical production. Qi *et al.* reported a GO-based nanochannel membrane with an interlayer channel size between water and methanol molecules, which can effectively separate methanol-water mixtures with a high separation efficiency of 99.89 wt.% [Figure 10B]^[163]. For a better comparison of related membranes, a summary of liquid molecular separation membranes is shown in Table 2.

Gas separation

Unlike other separations, gas separation is more sensitive to adsorption and desorption on membrane surfaces, requiring smaller nanochannels than other separation systems used throughout many industries, such as methane reforming, CO₂ capture, and hydrogen purification. Therefore, Controlling the nanochannel size and modifying the surface is essential.

The preparation of high-performance hydrogen purification membranes has become critical for constraining hydrogen energy to replace fossil dyes in catalytic hydrogen production processes. Ding *et al.* prepared a two-position separation membrane with a nanochannel size ~ 0.35 nm, which possesses H₂

Table 2. Summary of liquid molecular separation membranes

Membrane	Base material	Assembly method	Interlayer spacing	Molecular	Dye rejection (%)	Permeate flux (L·m ⁻² ·h ⁻¹ ·bar ⁻¹)
uGNMs ^[103]	Graphene	Vacuum filtration	sub-1-nm	DR 8,	> 99	21.8
PRGO/HNTs ^[182]	Graphene oxide	Solvent evaporation	8.87 Å	RB 5,	97.9	11.3
GO(120) NFM ^s ^[183]	Graphene oxide	Electro spraying	0.818 nm	EB,	99.99	11.13
c-GO/PAN ^[14]	Graphene oxide	Vacuum filtration	7.6/7.15 Å	DR 80,	> 99	78.5-117.2
MCM0.6-75 ^[184]	MXene	Suction filtration	1.41 nm	Methylene blue,	100	44.97
HGM30 ^[185]	Graphene oxide	Vacuum filtration	0.77 nm	rhodamine B (RhB),	99.30	89.6
MXene/GO-B ^[186]	MXene & graphene oxide	Vacuum filtration	5 Å	Brilliant blue,	100	0.23
GO/MXene ^[187]	Graphene oxide & MXene	Filtration	7.3 Å-14.5 Å	Chrysoidine G,	- 97	71.9
MXene/GO ^[188]	MXene & graphene oxide	Vacuum filtration	12.7 Å	Methylene blue,	98.56	16.69
10%MXene@CA ^[189]	MXene)/cellulose acetate	Casting	~ 6.68 Å	Rhodamine B,	92	256
21% Ag@MXene ^[190]	MXene	Vacuum filtration	2.1 Å	Rhodamine B,	79.93	420

permeability of > 2,200 Barrer and H₂/CO₂ selectivity of > 160, demonstrating excellent eventual commercialization potential [Figure 10C]^[164]. Carbon neutrality has become a hot topic in recent years. The separation of CO₂/N₂ is a prerequisite for CO₂ capture, leading to the successful synthesis of organic matter from CO₂. Zhou *et al.* cross-linked piperazine with GO, resulting in a membrane with a high affinity for CO₂, thus significantly improving the separation efficiency of CO₂/N₂ [Figure 10D]^[165]. The separation of hydrogen isotopes is vital for medical diagnosis and treatment. Lozada-Hidalgo *et al.* reported that graphene monolayers and BN membranes could separate hydrogen ion isotopes with a separation factor of about 10^[166]. For a better comparison of related membranes, a summary of gas separation membranes is shown in Table 3.

Ion sieving

Recently, researchers have paid increasing attention to high-performance ion sieve membranes in addition to traditional separation methods. Membranes with various properties are required to meet the different needs of ion sieve membranes for applications such as water desalination, microcurrent, hydrogen production, and energy storage.

In seawater desalination, stringent channel dimensions are necessary, with nanochannels often needing to be sub-nanometers in size to achieve ultra-high desalination efficiency. Chen *et al.* reported a graphene desalination membrane with sub-nanopores that achieved 99.99% NaCl rejection with an ultrafast water flux combined with evaporation methods [Figure 10E]^[167]. In energy storage applications, ion sieve membranes are often used as diaphragms, where excellent ionic conductivity and electrical insulation are required. Ghazi *et al.* synthesize a MoS₂/celgard separator with outstanding lithium ion passage and polysulfide retention capacity, which can effectively inhibit the shuttle effect in lithium-sulfur batteries, significantly improving the battery performance^[168].

Table 3. Summary of gas separation membranes

Membrane	Base material	Assembly method	Pore size	Gas	Selectivity
Graphene/NPC/MWNT ^[191]	Graphene	Spin-coating	20-30 nm	H ₂ /CH ₄	11-23
pCN ^[192]	Carbon nitride	Low-pressure chemical vapor deposition	N/A	H ₂ /CO ₂	6.58
Zn/Co-HDS ^[193]	Bimetallic MOF nanosheet	Vapor phase transformation	0.21 nm	H ₂ /CO ₂	54.1
β-ketoenamine-type COF membrane ^[194]	β-ketoenamine-type COF	Hot-drop coating	0.6 nm	H ₂ /CO ₂	22
(LDH/FAS)n-PDMS hybrid membranes	LDHs	Vacuum filtration/layer-by-layer assembly	N/A	H ₂ /CO ₂	43
BN membrane ^[195]	Boron nitride	Vacuum filtration	0.33 nm	Ethylene/Ethane	128
Printed GO-based membranes ^[196]	GO	Printing	0.89 nm	CO ₂ /N ₂	70

Yang *et al.* prepared a metal-organic framework as a multifunctional ionic sieve membrane for aqueous zinc-iodide batteries, greatly extending the battery lifespan^[169]. The recovery of rare metals has become increasingly popular due to the rising popularity of electric vehicles and electronic products. Efficient screening of metal ions is the key to recovering rare metals. Xu *et al.* developed a special lithium ion sieving UiO-67/AAO membrane, which achieved an ultra-high Li⁺ permeability of 27.01 mol m⁻² h⁻¹ and a Li⁺/Mg²⁺ selectivity of up to 159.4 [Figure 10F]^[170]. For a better comparison of related membranes, a summary of ion sieving membranes is shown in Table 4.

Important factors to consider when selecting a 2D nanochannel membrane for separation are the object to be separated, expected performance, ideal structure, cost-effectiveness, and environmental impact. In various application scenarios, choosing the appropriate membrane fabrication and modification process is the precondition for the membrane to ensure the ideal performance. Taking these factors into account can lead to the successful development of efficient and environmentally friendly separation processes.

CONCLUSION AND OUTLOOK

In summary, the emergence of a family of 2D materials with atomic-level thickness and excellent physical and chemical properties has brought significant development opportunities to nanochannel membranes. Over decades of development, 2D-materials-based membranes have made a preliminary breakthrough from raw materials to laboratory-level applications.

As outlined in Figure 11, this review summarized in detail strategies for constructing nanochannels in section CONSTRUCTING NANOCHANNELS WITH 2D NANOSHEETS. The extensive research on the swelling mechanism of 2D-material-based membranes has provided effective guidance for researchers to synthesize 2D nanosheets with ideal properties *via* “top-down” and “bottom-up” strategies, i.e., from a “clay” to “bricks” process. The appearance of various types of perforation methods (e.g., focused ion beam, plasma etching, chemical etching, *etc.*) has facilitated the transition from “bricks” to “porous bricks”, providing more options for the next step of nanochannel formation. The membrane assembly process is analogous

Table 4. Summary of ion sieving membranes

Membrane	Base material	Assembly method	Pore size	Ion/Ion	Selectivity
COF (TpBDMe ₂) membrane ^[197]	COF	Interfacial growth strategy	1.4 nm	K ⁺ /Mg ²⁺	765
COF-300/PS membrane ^[198]	COF-300 and polystyrene (PS)	N/A	1 nm	K ⁺ /Li ⁺	31.5
GOM ^[199]	GO	Vacuum filtration	13.9 Å	Lanthanides/actinides	~ 400
C@TM ^[200]	Ti ₃ C ₂ T _x	Suction-filtered	4.8 ± 0.1 Å	Li ⁺ /Mg ²⁺	30
EDA-GO ^[201]	GO	Vacuum filtration	5.82 Å-6.04 Å	K ⁺ /Na ⁺	1.5-5
s-MOF-801 polycrystalline ^[202]	MOF-801	Secondary growth method	6.2 Å	H ⁺ /V	194
COF-based membrane ^[203]	COF	Interfacial polymerization	2.34 nm	Li ⁺ /Mg ²⁺	64
GPETNC ^[204]	graphene	Asymmetric track-etching technique		K ⁺ /ions	4.6
KCl-controlled GO membranes ^[205]	GO	Vacuum filtration	10.7 Å	Na ⁺ /Mg ²⁺	30.6

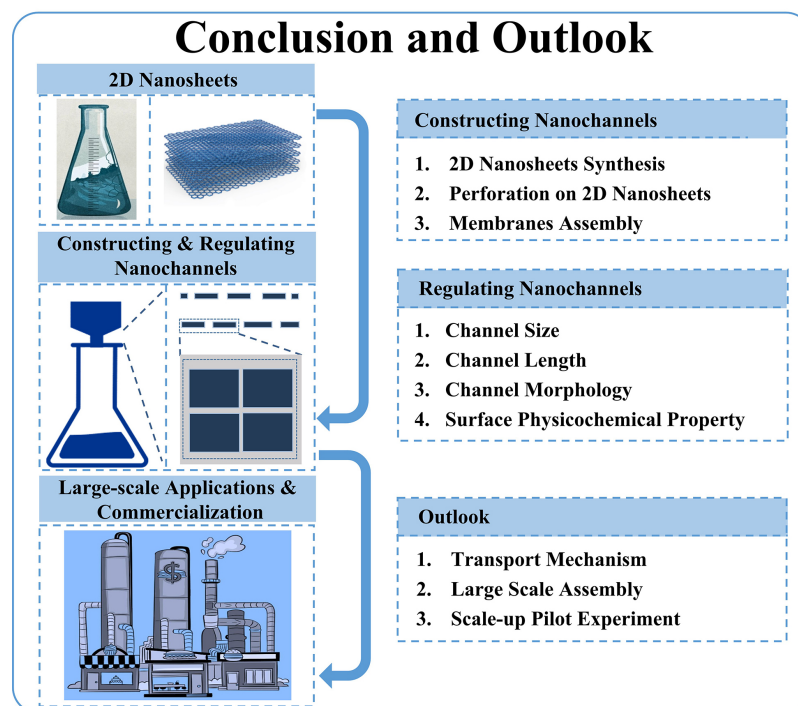


Figure 11. Conclusion and outlook of the development of the 2D-material-based membranes from the preparation of starting materials 2D nanosheets, the strategies of constructing nanochannels, the strategies of regulating the characteristics of nanochannels (channel size, channel length, channel morphology, and channel surface physicochemical properties), and the outlook to eventual commercialization.

to the process of “bricks” to “house”, and the selection of assembly strategy (e.g., pressure/vacuum filtration, spin coating, *etc.*) is crucial, as a suitable assembly method often leads to the right membrane.

A well-renovated and furnished “house” holds great value. Modifying the nanochannel of the membranes is similar to the “renovation” process. We comprehensively summarized the regulation strategies from four modifiable nanochannel properties, i.e., channel size, channel length, channel morphology, and the surface chemical property, in Section “REGULATING NANOCHANNELS”. The appropriate regulating strategy

allows the membrane to obtain the desired properties (e.g., defined size nanochannels, specific ionic or electronic conductivity, *etc.*) to meet the requirements for the corresponding applications.

Although researchers have tried a variety of membranes for liquid molecular separation, gas separation, and ion sieving applications (e.g., wastewater treatment, desalination, CO₂ capture, ion recovery, *etc.*), as we summarized in section APPLICATIONS OF 2D-MATERIAL-BASED NANOCHANNEL MEMBRANES, the vast majority of these applications are only at the laboratory level (“trial residence” stage), and the research and development of high-performance 2D-material-based nanochannel membranes are still at an early stage with both opportunities and challenges. To speed up the eventual commercialization of membranes and make them better serve the development of society, we propose an outlook on the future development of membranes from the following three aspects.

(1) Transport Mechanism. The current research has well explained the mechanism of the swelling problem and the construction and modification of nanochannels. Moreover, there is a large amount of work using theoretical calculations and simulations to try to make theoretical explanations for the differences in the filtration performance of various membranes. However, mechanisms during filtrations (e.g., the behavior mechanism of nanofluid in the channel, the rejection and passage mechanism of nanochannel to various filtrates, the force mechanism of nanochannel, the interaction mechanism between nanochannel and various filtrates, *etc.*) still need to be studied in depth. The emergence of various advanced characterization tools (e.g., cryoelectron microscopy, *in-situ* electron microscopy, *in-situ* Raman, *etc.*) provides new possibilities to investigate these mechanisms in depth. Mechanistic studies of the dynamic behavior of nanochannel membranes (including nanofluids and membranes themselves) will significantly advance mechanical innovation in the membrane field and accelerate the development of the new generation of high-performance membranes and industrial applications.

(2) Large-scale preparation. Rapid advances in chemistry and materials science have given rise to thousands of 2D materials. Yet, the mainstream “top-down” and “bottom-up” strategies are often only suitable for small-scale production in the laboratory. While there have been reports of kilogram-scale yields, this remains insufficient to meet the industrial demand of tens or even hundreds of kilograms. To overcome this challenge, it is crucial to develop new reliable methods for the preparation of 2D materials and reliable related manufacturing equipment. Notably, corresponding membrane assembly and modification technologies are also growing rapidly. Similarly, most methods, such as vacuum filtration, spin coating, and cross-linking, are more suitable for small-scale laboratory production and modification. Therefore, large-scale preparation is inevitable to apply advanced nanochannel membranes in the industry successfully. This calls for deep collaboration between the scientific and industrial communities to develop simple and scalable membrane fabrication methods, and relevant pilot experiments are necessary.

(3) Applications. Although almost all studies reported outstanding application performance, such as high selectivity, high permeability, and long membrane lifespan, these properties may be overestimated due to the limited membrane operating area, mild test conditions, and relatively short test durations in the laboratory. To truly reflect membrane capabilities, scaled-up application experiments under harsh conditions close to real-world applications (e.g., the effects of biochemical contaminants, sudden changes in water temperature and flow rate, *etc.*) are needed, which may pose additional challenges to researchers but will significantly facilitate the eventual commercialization of the membranes.

By addressing these challenges, the development of membranes with optimized nanochannels has the potential to transcend the limitations of traditional separation methods. Advances in membrane technology,

including selective ion, molecular, and particle transport, have important implications for energy-efficient operation, resource conservation, carbon capture, biogas purification, green hydrogen production, and energy storage. This avenue of research offers great promise for shaping a cleaner, more sustainable world.

DECLARATIONS

Authors' contributions

Draft writing, literature summary, picture production, language polishing, format adjustment: Xing C

Article frame writing, draft writing, literature summary: Zhang M

Literature summary, picture production: Liu L

Format adjustment: Zheng Z

Language polishing, format adjustment, literature summary: Zhou M

Financial support, article frame writing, language polishing: Liu C

Financial support, article frame writing, language polishing, supervision: Zhang S

Availability of data and materials

Not applicable.

Financial support and sponsorship

This research was supported by Griffith University Ph.D. Scholarship, the National Natural Science Foundation of China (Nos. 22274117 and 22008182), the Natural Science Foundation of Guangdong Province (No. 2021A1515010376), and the Education Department of Guangdong Province (No. 2020ZDZX2015).

Conflicts of interest

All authors declared that there are no conflicts of interest.

Ethical approval and consent to participate

Not applicable.

Consent for publication

Not applicable.

Copyright

© The Author(s) 2023.

REFERENCES

1. Wang F, Zhang Z, Shakir I, Yu C, Xu Y. 2D polymer nanosheets for membrane separation. *Adv Sci* 2022;9:e2103814. [DOI](#) [PubMed](#) [PMC](#)
2. Yuan S, Li X, Zhu J, Zhang G, Van Puyvelde P, Van der Bruggen B. Covalent organic frameworks for membrane separation. *Chem Soc Rev* 2019;48:2665-81. [DOI](#)
3. Li X, Liu Y, Wang J, Gascon J, Li J, Van der Bruggen B. Metal-organic frameworks based membranes for liquid separation. *Chem Soc Rev* 2017;46:7124-44. [DOI](#)
4. Park HB, Kamcev J, Robeson LM, Elimelech M, Freeman BD. Maximizing the right stuff: the trade-off between membrane permeability and selectivity. *Science* 2017;356:eaab0530. [DOI](#) [PubMed](#)
5. Wang S, Yang L, He G, et al. Two-dimensional nanochannel membranes for molecular and ionic separations. *Chem Soc Rev* 2020;49:1071-89. [DOI](#)
6. Kim JH, Choi Y, Kang J, et al. Shear-induced assembly of high-aspect-ratio graphene nanoribbon nanosheets in a confined microchannel: Membrane fabrication for ultrafast organic solvent nanofiltration. *Carbon* 2022;191:563-70. [DOI](#)
7. Pakulski D, Czepa W, Buffa SD, Ciesielski A, Samori P. Atom-thick membranes for water purification and blue energy harvesting. *Adv Funct Mater* 2020;30:1902394. [DOI](#)
8. Feng X, Peng D, Zhu J, Wang Y, Zhang Y. Recent advances of loose nanofiltration membranes for dye/salt separation. *Sep Purif*

- Technol* 2022;285:120228. DOI
9. Liu X, Jiang B, Yin X, Ma H, Hsiao BS. Highly permeable nanofibrous composite microfiltration membranes for removal of nanoparticles and heavy metal ions. *Sep Purif Technol* 2020;233:115976. DOI
 10. Ren Y, Ma Y, Min G, Zhang W, Lv L, Zhang W. A mini review of multifunctional ultrafiltration membranes for wastewater decontamination: additional functions of adsorption and catalytic oxidation. *Sci Total Environ* 2021;762:143083. DOI
 11. Zhao S, Liao Z, Fane A, et al. Engineering antifouling reverse osmosis membranes: a review. *Desalination* 2021;499:114857. DOI
 12. Xing C, Liu L, Guo X, et al. Efficient water purification using stabilized MXene nanofiltration membrane with controlled interlayer spacings. *Sep Purif Technol* 2023;317:123774. DOI
 13. Xing C, Liu C, Lai C, Zhang S. Tuning d-spacing of graphene oxide nanofiltration membrane for effective dye/salt separation. *Rare Met* 2023;42:418-29. DOI
 14. Xing C, Han J, Pei X, et al. Tunable graphene oxide nanofiltration membrane for effective dye/salt separation and desalination. *ACS Appl Mater Interfaces* 2021;13:55339-48. DOI
 15. Surwade SP, Smirnov SN, Vlassiuk IV, et al. Water desalination using nanoporous single-layer graphene. *Nat Nanotechnol* 2015;10:459-64. DOI
 16. Joshi RK, Carbone P, Wang FC, et al. Precise and ultrafast molecular sieving through graphene oxide membranes. *Science* 2014;343:752-4. DOI
 17. Ding L, Wei Y, Wang Y, Chen H, Caro J, Wang H. A two-dimensional lamellar membrane: MXene nanosheet stacks. *Angew Chem Int Ed* 2017;56:1825-9. DOI
 18. Caglar M, Silkina I, Brown BT, et al. Tunable anion-selective transport through monolayer graphene and hexagonal boron nitride. *ACS Nano* 2020;14:2729-38. DOI PubMed PMC
 19. Wang Y, Li L, Wei Y, et al. Water transport with ultralow friction through partially exfoliated g-C₃N₄ nanosheet membranes with self-supporting spacers. *Angew Chem Int Ed* 2017;56:8974-80. DOI
 20. Ries L, Petit E, Michel T, et al. Enhanced sieving from exfoliated MoS₂ membranes via covalent functionalization. *Nat Mater* 2019;18:1112-7. DOI
 21. Jia P, Wen Q, Liu D, et al. Highly efficient ionic photocurrent generation through WS₂-based 2D nanofluidic channels. *Small* 2019;15:e1905355. DOI
 22. Lu P, Liu Y, Zhou T, Wang Q, Li Y. Recent advances in layered double hydroxides (LDHs) as two-dimensional membrane materials for gas and liquid separations. *J Membr Sci* 2018;567:89-103. DOI
 23. Jiang Z, Liu H, Ahmed SA, et al. Insight into ion transfer through the sub-nanometer channels in zeolitic imidazolate frameworks. *Angew Chem Int Ed* 2017;129:4845-9. DOI
 24. Li X, Zhang H, Wang P, et al. Fast and selective fluoride ion conduction in sub-1-nanometer metal-organic framework channels. *Nat Commun* 2019;10:2490. DOI PubMed PMC
 25. Kuehl VA, Yin J, Duong PHH, et al. A highly ordered nanoporous, two-dimensional covalent organic framework with modifiable pores, and its application in water purification and ion sieving. *J Am Chem Soc* 2018;140:18200-7. DOI
 26. Danda G, Drndić M. Two-dimensional nanopores and nanoporous membranes for ion and molecule transport. *Curr Opin Biotechnol* 2019;55:124-33. DOI PubMed
 27. Prozorovska L, Kidambi PR. State-of-the-art and future prospects for atomically thin membranes from 2D materials. *Adv Mater* 2018;30:e1801179. DOI
 28. Kim S, Wang H, Lee YM. 2D Nanosheets and their composite membranes for water, gas, and ion separation. *Angew Chem Int Ed* 2019;131:17674-89. DOI
 29. Kang Y, Xia Y, Wang H, Zhang X. 2D laminar membranes for selective water and ion transport. *Adv Funct Mater* 2019;29:1902014. DOI
 30. Koltanow AR, Huang J. Two-dimensional nanofluidics. *Science* 2016;351:1395-6. DOI PubMed
 31. Tan C, Cao X, Wu XJ, et al. Recent advances in ultrathin two-dimensional nanomaterials. *Chem Rev* 2017;117:6225-331. DOI
 32. Nicolosi V, Chhowalla M, Kanatzidis MG, Strano MS, Coleman JN. Liquid exfoliation of layered materials. *Science* 2013;340:1226419. DOI
 33. Novoselov KS, Geim AK, Morozov SV, et al. Electric field effect in atomically thin carbon films. *Science* 2004;306:666-9. DOI
 34. Novoselov KS, Jiang D, Schedin F, et al. Two-dimensional atomic crystals. *Proc Natl Acad Sci USA* 2005;102:10451-3. DOI PubMed PMC
 35. Paton KR, Varrla E, Backes C, et al. Scalable production of large quantities of defect-free few-layer graphene by shear exfoliation in liquids. *Nat Mater* 2014;13:624-30. DOI
 36. Coleman JN, Lotya M, O'Neill A, et al. Two-dimensional nanosheets produced by liquid exfoliation of layered materials. *Science* 2011;331:568-71. DOI
 37. Peng Y, Li Y, Ban Y, et al. Metal-organic framework nanosheets as building blocks for molecular sieving membranes. *Science* 2014;346:1356-9. DOI
 38. Achee TC, Sun W, Hope JT, et al. High-yield scalable graphene nanosheet production from compressed graphite using electrochemical exfoliation. *Sci Rep* 2018;8:14525. DOI PubMed PMC
 39. Wang X, Narita A, Müllen K. Precision synthesis versus bulk-scale fabrication of graphenes. *Nat Rev Chem* 2018;2:0100. DOI
 40. Naguib M, Mashtalir O, Carle J, et al. Two-dimensional transition metal carbides. *ACS Nano* 2012;6:1322-31. DOI

41. Wang Q, O'Hare D. Recent advances in the synthesis and application of layered double hydroxide (LDH) nanosheets. *Chem Rev* 2012;112:4124-55. DOI PubMed
42. Ma R, Sasaki T. Two-dimensional oxide and hydroxide nanosheets: controllable high-quality exfoliation, molecular assembly, and exploration of functionality. *Acc Chem Res* 2015;48:136-43. DOI PubMed
43. Varoon K, Zhang X, Elyassi B, et al. Dispersible exfoliated zeolite nanosheets and their application as a selective membrane. *Science* 2011;334:72-5. DOI
44. Ren J, Liu X, Zhang L, Liu Q, Gao R, Dai W. Thermal oxidative etching method derived graphitic C₃N₄: highly efficient metal-free catalyst in the selective epoxidation of styrene. *RSC Adv* 2017;7:5340-8. DOI
45. Yu J, Li J, Zhang W, Chang H. Synthesis of high quality two-dimensional materials via chemical vapor deposition. *Chem Sci* 2015;6:6705-16. DOI PubMed PMC
46. Shi Y, Li H, Li LJ. Recent advances in controlled synthesis of two-dimensional transition metal dichalcogenides via vapour deposition techniques. *Chem Soc Rev* 2015;44:2744-56. DOI
47. Ou M, Wang X, Yu L, et al. The emergence and evolution of borophene. *Adv Sci* 2021;8:2001801. DOI PubMed PMC
48. Huang S, Dakhchoune M, Luo W, et al. Single-layer graphene membranes by crack-free transfer for gas mixture separation. *Nat Commun* 2018;9:2632. DOI PubMed PMC
49. Zhang J, Lin L, Sun L, et al. Clean transfer of large graphene single crystals for high-intactness suspended membranes and liquid cells. *Adv Mater* 2017;29:1700639. DOI
50. Chen Y, Gong XL, Gai JG. Progress and challenges in transfer of large-area graphene films. *Adv Sci* 2016;3:1500343. DOI PubMed PMC
51. Jeon MY, Kim D, Kumar P, et al. Ultra-selective high-flux membranes from directly synthesized zeolite nanosheets. *Nature* 2017;543:690-4. DOI
52. Makiura R, Motoyama S, Umemura Y, Yamanaka H, Sakata O, Kitagawa H. Surface nano-architecture of a metal-organic framework. *Nat Mater* 2010;9:565-71. DOI PubMed
53. Rodenas T, Luz I, Prieto G, et al. Metal-organic framework nanosheets in polymer composite materials for gas separation. *Nat Mater* 2015;14:48-55. DOI PubMed PMC
54. Feng X, Ding X, Jiang D. Covalent organic frameworks. *Chem Soc Rev* 2012;41:6010-22. DOI PubMed
55. Dai W, Shao F, Szczerbiński J, et al. Synthesis of a two-dimensional covalent organic monolayer through dynamic imine chemistry at the air/water interface. *Angew Chem Int Ed* 2016;128:221-5. DOI
56. Kandambeth S, Biswal BP, Chaudhari HD, et al. Selective molecular sieving in self-standing porous covalent-organic-framework membranes. *Adv Mater* 2017;29:1603945. DOI
57. Moreno C, Vilas-Varela M, Kretz B, et al. Bottom-up synthesis of multifunctional nanoporous graphene. *Science* 2018;360:199-203. DOI
58. Fischbein MD, Drndić M. Electron beam nanosculpting of suspended graphene sheets. *Appl Phys Lett* 2008;93:113107. DOI
59. Koenig SP, Wang L, Pellegrino J, Bunch JS. Selective molecular sieving through porous graphene. *Nat Nanotechnol* 2012;7:728-32. DOI PubMed
60. Celebi K, Buchheim J, Wyss RM, et al. Ultimate permeation across atomically thin porous graphene. *Science* 2014;344:289-92. DOI
61. Russo CJ, Golovchenko JA. Atom-by-atom nucleation and growth of graphene nanopores. *Proc Natl Acad Sci USA* 2012;109:5953-7. DOI PubMed PMC
62. O'Hern SC, Boutilier MS, Idrobo JC, et al. Selective ionic transport through tunable subnanometer pores in single-layer graphene membranes. *Nano Lett* 2014;14:1234-41. DOI
63. Zhu Y, Murali S, Stoller MD, et al. Carbon-based supercapacitors produced by activation of graphene. *Science* 2011;332:1537-41. DOI
64. Zhang LL, Zhao X, Stoller MD, et al. Highly conductive and porous activated reduced graphene oxide films for high-power supercapacitors. *Nano Lett* 2012;12:1806-12. DOI
65. Zhao X, Hayner CM, Kung MC, Kung HH. Flexible holey graphene paper electrodes with enhanced rate capability for energy storage applications. *ACS Nano* 2011;5:8739-49. DOI PubMed
66. Wang X, Jiao L, Sheng K, Li C, Dai L, Shi G. Solution-processable graphene nanomeshes with controlled pore structures. *Sci Rep* 2013;3:1996. DOI PubMed PMC
67. Palaniselvam T, Valappil MO, Illathvalappil R, Kurungot S. Nanoporous graphene by quantum dots removal from graphene and its conversion to a potential oxygen reduction electrocatalyst via nitrogen doping. *Energy Environ Sci* 2014;7:1059. DOI
68. Zhou D, Cui Y, Xiao PW, Jiang MY, Han BH. A general and scalable synthesis approach to porous graphene. *Nat Commun* 2014;5:4716. DOI
69. Gilbert SM, Dunn G, Azizi A, et al. Fabrication of subnanometer-precision nanopores in hexagonal boron nitride. *Sci Rep* 2017;7:15096. DOI PubMed PMC
70. Feng J, Graf M, Liu K, et al. Single-layer MoS₂ nanopores as nanopower generators. *Nature* 2016;536:197-200. DOI
71. Feng J, Liu K, Graf M, et al. Electrochemical reaction in single layer MoS₂: nanopores opened atom by atom. *Nano Lett* 2015;15:3431-8. DOI
72. Geim AK, Grigorieva IV. Van der Waals heterostructures. *Nature* 2013;499:419-25. DOI
73. Radha B, Esfandiari A, Wang FC, et al. Molecular transport through capillaries made with atomic-scale precision. *Nature*

- 2016;538:222-5. DOI
74. Esfandiar A, Radha B, Wang FC, et al. Size effect in ion transport through angstrom-scale slits. *Science* 2017;358:511-3. DOI
75. Keerthi A, Geim AK, Janardanan A, et al. Ballistic molecular transport through two-dimensional channels. *Nature* 2018;558:420-4. DOI
76. Hu S, Lozada-Hidalgo M, Wang FC, et al. Proton transport through one-atom-thick crystals. *Nature* 2014;516:227-30. DOI
77. Gopinadhan K, Hu S, Esfandiar A, et al. Complete steric exclusion of ions and proton transport through confined monolayer water. *Science* 2019;363:145-8. DOI
78. Algara-Siller G, Lehtinen O, Wang FC, et al. Square ice in graphene nanocapillaries. *Nature* 2015;519:443-5. DOI
79. Fumagalli L, Esfandiar A, Fabregas R, et al. Anomalously low dielectric constant of confined water. *Science* 2018;360:1339-42. DOI
80. Mouterde T, Keerthi A, Poggioli AR, et al. Molecular streaming and its voltage control in ångström-scale channels. *Nature* 2019;567:87-90. DOI
81. Shen J, Liu G, Huang K, Chu Z, Jin W, Xu N. Subnanometer two-dimensional graphene oxide channels for ultrafast gas sieving. *ACS Nano* 2016;10:3398-409. DOI
82. Dikin DA, Stankovich S, Zimney EJ, et al. Preparation and characterization of graphene oxide paper. *Nature* 2007;448:457-60. DOI
83. Tsou C, An Q, Lo S, et al. Effect of microstructure of graphene oxide fabricated through different self-assembly techniques on 1-butanol dehydration. *J Membr Sci* 2015;477:93-100. DOI
84. Zhang M, Sun J, Mao Y, Liu G, Jin W. Effect of substrate on formation and nanofiltration performance of graphene oxide membranes. *J Membr Sci* 2019;574:196-204. DOI
85. Kim HW, Yoon HW, Yoon SM, et al. Selective gas transport through few-layered graphene and graphene oxide membranes. *Science* 2013;342:91-5. DOI
86. Chi C, Wang X, Peng Y, et al. Facile preparation of graphene oxide membranes for gas separation. *Chem Mater* 2016;28:2921-7. DOI
87. Guan K, Shen J, Liu G, Zhao J, Zhou H, Jin W. Spray-evaporation assembled graphene oxide membranes for selective hydrogen transport. *Sep Purif Technol* 2017;174:126-35. DOI
88. Ibrahim AF, Lin Y. Synthesis of graphene oxide membranes on polyester substrate by spray coating for gas separation. *Chem Eng Sci* 2018;190:312-9. DOI
89. Akbari A, Sheath P, Martin ST, et al. Large-area graphene-based nanofiltration membranes by shear alignment of discotic nematic liquid crystals of graphene oxide. *Nat Commun* 2016;7:10891. DOI PubMed PMC
90. Zhong J, Sun W, Wei Q, Qian X, Cheng HM, Ren W. Efficient and scalable synthesis of highly aligned and compact two-dimensional nanosheet films with record performances. *Nat Commun* 2018;9:3484. DOI PubMed PMC
91. Hu M, Mi B. Enabling graphene oxide nanosheets as water separation membranes. *Environ Sci Technol* 2013;47:3715-23. DOI PubMed
92. Hu M, Mi B. Layer-by-layer assembly of graphene oxide membranes via electrostatic interaction. *J Membr Sci* 2014;469:80-7. DOI
93. Song X, Zambare RS, Qi S, et al. Charge-gated ion transport through polyelectrolyte intercalated amine reduced graphene oxide membranes. *ACS Appl Mater Interfaces* 2017;9:41482-95. DOI
94. Zhao J, Zhu Y, Pan F, et al. Fabricating graphene oxide-based ultrathin hybrid membrane for pervaporation dehydration via layer-by-layer self-assembly driven by multiple interactions. *J Membr Sci* 2015;487:162-72. DOI
95. Zhao D, Chen Z, Liao X. Microstructural evolution and ferroelectricity in HfO₂ films. *Microstructures* 2022;2:2022007. DOI
96. Chen Z, Liao X, Zhang S. The visible hand behind properties. *Microstructures* 2021;1:2021001. DOI
97. Xing C, Chen H, Qian S, et al. Regulating liquid and solid-state electrolytes for solid-phase conversion in Li-S batteries. *Chem* 2022;8:1201-30. DOI
98. Xing C, Chen H, Zhang S. Powering 10-Ah-level Li-S pouch cell via a smart “skin”. *Matter* 2022;5:2523-5. DOI
99. Abraham J, Vasu KS, Williams CD, et al. Tunable sieving of ions using graphene oxide membranes. *Nat Nanotechnol* 2017;12:546-50. DOI
100. Li W, Wu W, Li Z. Controlling interlayer spacing of graphene oxide membranes by external pressure regulation. *ACS Nano* 2018;12:9309-17. DOI
101. Chen L, Shi G, Shen J, et al. Ion sieving in graphene oxide membranes via cationic control of interlayer spacing. *Nature* 2017;550:380-3. DOI
102. Qiu L, Zhang X, Yang W, Wang Y, Simon GP, Li D. Controllable corrugation of chemically converted graphene sheets in water and potential application for nanofiltration. *Chem Commun* 2011;47:5810-2. DOI
103. Han Y, Xu Z, Gao C. Ultrathin graphene nanofiltration membrane for water purification. *Adv Funct Mater* 2013;23:3693-700. DOI
104. Liu H, Wang H, Zhang X. Facile fabrication of freestanding ultrathin reduced graphene oxide membranes for water purification. *Adv Mater* 2015;27:249-54. DOI
105. Hung W, Tsou C, De Guzman M, et al. Cross-linking with diamine monomers to prepare composite graphene oxide-framework membranes with varying *d*-spacing. *Chem Mater* 2014;26:2983-90. DOI
106. Zhang M, Mao Y, Liu G, Liu G, Fan Y, Jin W. Molecular bridges stabilize graphene oxide membranes in water. *Angew Chem Int Ed* 2020;59:1689-95. DOI PubMed
107. Jia Z, Shi W. Tailoring permeation channels of graphene oxide membranes for precise ion separation. *Carbon* 2016;101:290-5. DOI
108. Lim M, Choi Y, Kim J, et al. Cross-linked graphene oxide membrane having high ion selectivity and antibacterial activity prepared

- using tannic acid-functionalized graphene oxide and polyethyleneimine. *J Membr Sci* 2017;521:1-9. DOI
109. Wang S, Wu Y, Zhang N, et al. A highly permeable graphene oxide membrane with fast and selective transport nanochannels for efficient carbon capture. *Energy Environ Sci* 2016;9:3107-12. DOI
110. Zhang P, Gong J, Zeng G, et al. Cross-linking to prepare composite graphene oxide-framework membranes with high-flux for dyes and heavy metal ions removal. *Chem Eng J* 2017;322:657-66. DOI
111. Xu XL, Lin FW, Du Y, Zhang X, Wu J, Xu ZK. Graphene oxide nanofiltration membranes stabilized by cationic porphyrin for high salt rejection. *ACS Appl Mater Inter* 2016;8:12588-93. DOI
112. Fei F, Cseri L, Szekely G, Blanford CF. Robust covalently cross-linked polybenzimidazole/graphene oxide membranes for high-flux organic solvent nanofiltration. *ACS Appl Mater Inter* 2018;10:16140-7. DOI
113. Yang J, Gong D, Li G, et al. Self-assembly of thiourea-crosslinked graphene oxide framework membranes toward separation of small molecules. *Adv Mater* 2018;30:e1705775. DOI
114. Liu Y, Xu L, Liu J, et al. Graphene oxides cross-linked with hyperbranched polyethylenimines: preparation, characterization and their potential as recyclable and highly efficient adsorption materials for lead (II) ions. *Chem Eng J* 2016;285:698-708. DOI
115. Nam YT, Choi J, Kang KM, Kim DW, Jung HT. Enhanced stability of laminated graphene oxide membranes for nanofiltration via interstitial amide bonding. *ACS Appl Mater Inter* 2016;8:27376-82. DOI
116. Wang N, Ji S, Zhang G, Li J, Wang L. Self-assembly of graphene oxide and polyelectrolyte complex nano hybrid membranes for nanofiltration and pervaporation. *Chem Eng J* 2012;213:318-29. DOI
117. Wang S, Xie Y, He G, et al. Graphene oxide membranes with heterogeneous nanodomains for efficient CO₂ separations. *Angew Chem Int Ed* 2017;56:14246-51. DOI
118. Ran J, Chu C, Pan T, et al. Non-covalent cross-linking to boost the stability and permeability of graphene-oxide-based membranes. *J Mater Chem A* 2019;7:8085-91. DOI
119. Wang W, Eftekhari E, Zhu G, Zhang X, Yan Z, Li Q. Graphene oxide membranes with tunable permeability due to embedded carbon dots. *Chem Commun* 2014;50:13089-92. DOI
120. Han Y, Jiang Y, Gao C. High-flux graphene oxide nanofiltration membrane intercalated by carbon nanotubes. *ACS Appl Mater Inter* 2015;7:8147-55. DOI
121. Goh K, Jiang W, Karahan HE, et al. All-carbon nanoarchitectures as high-performance separation membranes with superior stability. *Adv Funct Mater* 2015;25:7348-59. DOI
122. Zhang M, Guan K, Shen J, Liu G, Fan Y, Jin W. Nanoparticles@rGO membrane enabling highly enhanced water permeability and structural stability with preserved selectivity. *AIChE J* 2017;63:5054-63. DOI
123. Li C, Sun W, Lu Z, Ao X, Yang C, Li S. Systematic evaluation of TiO₂-GO-modified ceramic membranes for water treatment: retention properties and fouling mechanisms. *Chem Eng J* 2019;378:122138. DOI
124. Wang S, Mahalingam D, Sutisna B, Nunes SP. 2D-dual-spacing channel membranes for high performance organic solvent nanofiltration. *J Mater Chem A* 2019;7:11673-82. DOI
125. Guo H, Kong G, Yang G, et al. Cross-linking between sodalite nanoparticles and graphene oxide in composite membranes to trigger high gas permeance, selectivity, and stability in hydrogen separation. *Angew Chem Int Ed* 2020;132:6343-7. DOI
126. Guan K, Zhao D, Zhang M, et al. 3D nanoporous crystals enabled 2D channels in graphene membrane with enhanced water purification performance. *J Membr Sci* 2017;542:41-51. DOI
127. Li W, Zhang Y, Su P, et al. Metal-organic framework channelled graphene composite membranes for H₂/CO₂ separation. *J Mater Chem A* 2016;4:18747-52. DOI
128. Khan NA, Yuan J, Wu H, et al. Mixed nanosheet membranes assembled from chemically grafted graphene oxide and covalent organic frameworks for ultra-high water flux. *ACS Appl Mater Inter* 2019;11:28978-86. DOI
129. Sui X, Yuan Z, Liu C, et al. Graphene oxide laminates intercalated with 2D covalent-organic frameworks as a robust nanofiltration membrane. *J Mater Chem A* 2020;8:9713-25. DOI
130. Mao Y, Zhang M, Cheng L, et al. Bola-amphiphile-imidazole embedded GO membrane with enhanced solvent dehydration properties. *J Membr Sci* 2020;595:117545. DOI
131. Wang Z, Tu Q, Zheng S, Urban JJ, Li S, Mi B. Understanding the aqueous stability and filtration capability of MoS₂ membranes. *Nano Lett* 2017;17:7289-98. DOI PubMed
132. Ran J, Pan T, Wu Y, et al. Endowing g-C₃N₄ membranes with superior permeability and stability by using acid spacers. *Angew Chem Int Ed* 2019;58:16463-8. DOI
133. Wang J, Zhang Z, Zhu J, et al. Ion sieving by a two-dimensional Ti₃C₂T_x alginate lamellar membrane with stable interlayer spacing. *Nat Commun* 2020;11:3540. DOI PubMed PMC
134. Cohen-Tanugi D, Grossman JC. Water desalination across nanoporous graphene. *Nano Lett* 2012;12:3602-8. DOI PubMed
135. Yang Q, Su Y, Chi C, et al. Ultrathin graphene-based membrane with precise molecular sieving and ultrafast solvent permeation. *Nat Mater* 2017;16:1198-202. DOI
136. Li H, Song Z, Zhang X, et al. Ultrathin, molecular-sieving graphene oxide membranes for selective hydrogen separation. *Science* 2013;342:95-8. DOI
137. Heiraniyan M, Farimani AB, Aluru NR. Water desalination with a single-layer MoS₂ nanopore. *Nat Commun* 2015;6:8616. DOI PubMed PMC
138. Yang Y, Yang X, Liang L, et al. Large-area graphene-nanomesh/carbon-nanotube hybrid membranes for ionic and molecular

- nanofiltration. *Science* 2019;364:1057-62. DOI
139. Ibrahim A, Lin Y. Gas permeation and separation properties of large-sheet stacked graphene oxide membranes. *J Membr Sci* 2018;550:238-45. DOI
140. Amadei CA, Montessori A, Kadow JP, Succi S, Vecitis CD. Role of oxygen functionalities in graphene oxide architectural laminate subnanometer spacing and water transport. *Environ Sci Technol* 2017;51:4280-8. DOI PubMed
141. Chen J, Li Y, Huang L, Jia N, Li C, Shi G. Size Fractionation of graphene oxide sheets via filtration through track-etched membranes. *Adv Mater* 2015;27:3654-60. DOI
142. Shen J, Zhang M, Liu G, Guan K, Jin W. Size effects of graphene oxide on mixed matrix membranes for CO₂ separation. *AIChE J* 2016;62:2843-52. DOI
143. Geng H, Yao B, Zhou J, et al. Size fractionation of graphene oxide nanosheets via controlled directional freezing. *J Am Chem Soc* 2017;139:12517-23. DOI
144. Sun P, Zheng F, Zhu M, et al. Selective trans-membrane transport of alkali and alkaline earth cations through graphene oxide membranes based on cation- π interactions. *ACS Nano* 2014;8:850-9. DOI
145. Nie L, Goh K, Wang Y, et al. Realizing small-flake graphene oxide membranes for ultrafast size-dependent organic solvent nanofiltration. *Sci Adv* 2020;6:eaa9184. DOI PubMed PMC
146. Ying Y, Sun L, Wang Q, Fan Z, Peng X. In-plane mesoporous graphene oxide nanosheet assembled membranes for molecular separation. *RSC Adv* 2014;4:21425. DOI
147. Li Y, Zhao W, Weyland M, et al. Thermally reduced nanoporous graphene oxide membrane for desalination. *Environ Sci Technol* 2019;53:8314-23. DOI
148. Peng Y, Li Y, Ban Y, Yang W. Two-dimensional metal-organic framework nanosheets for membrane-based gas separation. *Angew Chem Int Ed* 2017;129:9889-93. DOI
149. Shinde DB, Sheng G, Li X, et al. Crystalline 2D covalent organic framework membranes for high-flux organic solvent nanofiltration. *J Am Chem Soc* 2018;140:14342-9. DOI
150. Xi Y, Liu Z, Ji J, et al. Graphene-based membranes with uniform 2D nanochannels for precise sieving of mono-/multi-valent metal ions. *J Membr Sci* 2018;550:208-18. DOI
151. Li Y, Yuan S, Xia Y, et al. Mild annealing reduced graphene oxide membrane for nanofiltration. *J Membr Sci* 2020;601:117900. DOI
152. Saraswat V, Jacobberger RM, Ostrander JS, et al. Invariance of water permeance through size-differentiated graphene oxide laminates. *ACS Nano* 2018;12:7855-65. DOI
153. Kang Y, Qiu R, Jian M, et al. The role of nanowrinkles in mass transport across graphene-based membranes. *Adv Funct Mater* 2020;30:2003159. DOI
154. Huang H, Song Z, Wei N, et al. Ultrafast viscous water flow through nanostrand-channelled graphene oxide membranes. *Nat Commun* 2013;4:2979. DOI
155. Sun L, Ying Y, Huang H, et al. Ultrafast molecule separation through layered WS₂ nanosheet membranes. *ACS Nano* 2014;8:6304-11. DOI
156. Park S, Lee KS, Bozoklu G, Cai W, Nguyen ST, Ruoff RS. Graphene oxide papers modified by divalent ions-enhancing mechanical properties via chemical cross-linking. *ACS Nano* 2008;2:572-8. DOI
157. Ding L, Li L, Liu Y, et al. Effective ion sieving with Ti₃C₂T_x MXene membranes for production of drinking water from seawater. *Nat Sustain* 2020;3:296-302. DOI
158. Kim S, Lin X, Ou R, et al. Highly crosslinked, chlorine tolerant polymer network entwined graphene oxide membrane for water desalination. *J Mater Chem A* 2017;5:1533-40. DOI
159. Kim S, Ou R, Hu Y, et al. Non-swelling graphene oxide-polymer nanocomposite membrane for reverse osmosis desalination. *J Membr Sci* 2018;562:47-55. DOI
160. Xie X, Chen C, Zhang N, Tang Z, Jiang J, Xu Y. Microstructure and surface control of MXene films for water purification. *Nat Sustain* 2019;2:856-62. DOI
161. Alkhouzaam A, Qiblawey H, Khraisheh M. Polydopamine functionalized graphene oxide as membrane nanofiller: spectral and structural studies. *Membranes* 2021;11:86. DOI PubMed PMC
162. Xing C, Zhang Y, Huang R, et al. Anti-swelling polyethyleneimine-modified MXene nanofiltration membranes for efficient and selective molecular separation. *EcoMat* 2023;5:e12300. DOI
163. Qi B, He X, Zeng G, et al. Strict molecular sieving over electrodeposited 2D-interspacing-narrowed graphene oxide membranes. *Nat Commun* 2017;8:825. DOI PubMed PMC
164. Ding L, Wei Y, Li L, et al. MXene molecular sieving membranes for highly efficient gas separation. *Nat Commun* 2018;9:155. DOI PubMed PMC
165. Zhou F, Tien HN, Xu WL, et al. Ultrathin graphene oxide-based hollow fiber membranes with brush-like CO₂-philic agent for highly efficient CO₂ capture. *Nat Commun* 2017;8:2107. DOI PubMed PMC
166. Lozada-Hidalgo M, Hu S, Marshall O, et al. Sieving hydrogen isotopes through two-dimensional crystals. *Science* 2016;351:68-70. DOI
167. Chen X, Zhu Y, Yu H, et al. Ultrafast water evaporation through graphene membranes with subnanometer pores for desalination. *J Membr Sci* 2021;621:118934. DOI

168. Ghazi ZA, He X, Khattak AM, et al. MoS₂/Celgard separator as efficient polysulfide barrier for long-life lithium-sulfur batteries. *Adv Mater* 2017;29:1606817. DOI
169. Yang H, Qiao Y, Chang Z, Deng H, He P, Zhou H. A metal-organic framework as a multifunctional ionic sieve membrane for long-life aqueous zinc-iodide batteries. *Adv Mater* 2020;32:e2004240. DOI
170. Xu R, Kang Y, Zhang W, Zhang X, Pan B. Oriented UiO-67 metal-organic framework membrane with fast and selective lithium-ion transport. *Angew Chem Int Ed* 2022;61:e202115443. DOI
171. Bonaccorso F, Lombardo A, Hasan T, Sun Z, Colombo L, Ferrari AC. Production and processing of graphene and 2D crystals. *Mater Today* 2012;15:564-89. DOI
172. Navik R, Gai Y, Wang W, Zhao Y. Curcumin-assisted ultrasound exfoliation of graphite to graphene in ethanol. *Ultrason Sonochem* 2018;48:96-102. DOI PubMed
173. Dhanabalan SC, Ponraj JS, Guo Z, Li S, Bao Q, Zhang H. Emerging trends in phosphorene fabrication towards next generation devices. *Adv Sci* 2017;4:1600305. DOI PubMed PMC
174. Batool S, Idrees M, Zhang SR, Han ST, Zhou Y. Novel charm of 2D materials engineering in memristor: when electronics encounter layered morphology. *Nanoscale Horiz* 2022;7:480-507. DOI
175. Duraisamy S, Ganguly A, Sharma PK, Benson J, Davis J, Papakonstantinou P. One-step hydrothermal synthesis of phase-engineered MoS₂/MoO₃ electrocatalysts for hydrogen evolution reaction. *ACS Appl Nano Mater* 2021;4:2642-56. DOI
176. Miao Y, Tsapatsis M. Electron beam patterning of metal-organic frameworks. *Chem Mater* 2021;33:754-60. DOI
177. Lu X, Wang R, Hao L, et al. Oxidative etching of MoS₂/WS₂ nanosheets to their QDs by facile UV irradiation. *Phys Chem Chem Phys* 2016;18:31211-6. DOI
178. Wei Y, Pastuovic Z, Shen C, Murphy T, Gore DB. Ion beam engineered graphene oxide membranes for mono-/di-valent metal ions separation. *Carbon* 2020;158:598-606. DOI
179. Kim B, Im S, Yoo G. Performance evaluation of CNN-based end-point detection using in-situ plasma etching data. *Electronics* 2021;10:49. DOI
180. Huang X, Cen D, Wei R, Fan H, Bao Z. Synthesis of porous Si/C composite nanosheets from vermiculite with a hierarchical structure as a high-performance anode for lithium-ion battery. *ACS Appl Mater Inter* 2019;11:26854-62. DOI
181. Pasquarelli RM, Ginley DS, O'Hayre R. Solution processing of transparent conductors: from flask to film. *Chem Soc Rev* 2011;40:5406-41. DOI PubMed
182. Zhu L, Wang H, Bai J, Liu J, Zhang Y. A porous graphene composite membrane intercalated by halloysite nanotubes for efficient dye desalination. *Desalination* 2017;420:145-57. DOI
183. Chen L, Moon J, Ma X, et al. High performance graphene oxide nanofiltration membrane prepared by electrospraying for wastewater purification. *Carbon* 2018;130:487-94. DOI
184. Zhang S, Liao S, Qi F, et al. Direct deposition of two-dimensional MXene nanosheets on commercially available filter for fast and efficient dye removal. *J Hazard Mater* 2020;384:121367. DOI
185. Han R, Wu P. High-performance graphene oxide nanofiltration membrane with continuous nanochannels prepared by the *in situ* oxidation of MXene. *J Mater Chem A* 2019;7:6475-81. DOI
186. Kang KM, Kim DW, Ren CE, et al. Selective molecular separation on Ti₃C₂T_x-graphene oxide membranes during pressure-driven filtration: comparison with graphene oxide and MXenes. *ACS Appl Mater Inter* 2017;9:44687-94. DOI
187. Liu T, Liu X, Graham N, Yu W, Sun K. Two-dimensional MXene incorporated graphene oxide composite membrane with enhanced water purification performance. *J Membr Sci* 2020;593:117431. DOI
188. Wei S, Xie Y, Xing Y, et al. Two-dimensional graphene Oxide/MXene composite lamellar membranes for efficient solvent permeation and molecular separation. *J Membr Sci* 2019;582:414-22. DOI
189. Pandey RP, Rasheed PA, Gomez T, Azam RS, Mahmoud KA. A fouling-resistant mixed-matrix nanofiltration membrane based on covalently cross-linked Ti₃C₂T_x (MXene)/cellulose acetate. *J Membr Sci* 2020;607:118139. DOI
190. Pandey RP, Rasool K, Madhavan VE, Aïssa B, Gogotsi Y, Mahmoud KA. Ultrahigh-flux and fouling-resistant membranes based on layered silver/MXene (Ti₃C₂T_x) nanosheets. *J Mater Chem A* 2018;6:3522-33. DOI
191. Lee W, Bondaz L, Huang S, He G, Dakhchoune M, Agrawal KV. Centimeter-scale gas-sieving nanoporous single-layer graphene membrane. *J Membr Sci* 2021;618:118745. DOI
192. Ashirov T, Siena JS, Zhang M, Ozgur Yazaydin A, Antonietti M, Coskun A. Fast light-switchable polymeric carbon nitride membranes for tunable gas separation. *Nat Commun* 2022;13:7299. DOI PubMed PMC
193. Ma C, Gao G, Liu H, Liu Y, Zhang X. Fabrication of 2D bimetallic metal-organic framework ultrathin membranes by vapor phase transformation of hydroxy double salts. *J Membr Sci* 2022;644:120167. DOI
194. Wang P, Peng Y, Zhu C, et al. Single-phase covalent organic framework staggered stacking nanosheet membrane for CO₂-selective separation. *Angew Chem Int Ed* 2021;60:19047-52. DOI
195. Dou H, Jiang B, Xu M, et al. Boron nitride membranes with a distinct nanoconfinement effect for efficient ethylene/ethane separation. *Angew Chem Int Ed* 2019;131:14107-13. DOI
196. Zhou F, Dong Q, Chen J, et al. Printed graphene oxide-based membranes for gas separation and carbon capture. *Chem Eng J* 2022;430:132942. DOI
197. Sheng F, Wu B, Li X, et al. Efficient ion sieving in covalent organic framework membranes with sub-2-nanometer channels. *Adv Mater* 2021;33:e2104404. DOI

198. Niu B, Xin W, Qian Y, Kong XY, Jiang L, Wen L. Covalent organic frameworks embedded in polystyrene membranes for ion sieving. *Chem Commun* 2022;58:5403-6. [DOI](#) [PubMed](#)
199. Wang Z, Huang L, Dong X, et al. Ion sieving in graphene oxide membrane enables efficient actinides/lanthanides separation. *Nat Commun* 2023;14:261. [DOI](#) [PubMed](#) [PMC](#)
200. He M, Liu Z, Wang L, et al. Carboxymethylcellulose (CMC)/glutaraldehyde (GA)-modified $Ti_3C_2T_x$ membrane and its efficient ion sieving performance. *J Membr Sci* 2023;675:121541. [DOI](#)
201. Leong ZY, Han Z, Wang G, Li D, Yang SA, Yang HY. Electric field modulated ion-sieving effects of graphene oxide membranes. *J Mater Chem A* 2021;9:244-53. [DOI](#)
202. Cao H, Xia Y, Lu Y, et al. MOF-801 polycrystalline membrane with sub-10 nm polymeric assembly layer for ion sieving and flow battery storage. *AIChE J* 2022;68:e17657. [DOI](#)
203. Bing S, Xian W, Chen S, et al. Bio-inspired construction of ion conductive pathway in covalent organic framework membranes for efficient lithium extraction. *Matter* 2021;4:2027-38. [DOI](#)
204. Su S, Zhang Y, Peng S, et al. Multifunctional graphene heterogeneous nanochannel with voltage-tunable ion selectivity. *Nat Commun* 2022;13:4894. [DOI](#) [PubMed](#) [PMC](#)
205. Liang S, Wang S, Chen L, Fang H. Controlling interlayer spacings of graphene oxide membranes with cationic for precise sieving of mono-/multi-valent ions. *Sep Purif Technol* 2020;241:116738. [DOI](#)